

Spatially heterogeneous post-Caledonian burial and exhumation across the Scottish Highlands

Michelle L. Fame¹, James A. Spotila¹, Lewis A. Owen², Jason M. Dortch³, and David L. Shuster^{4,5}

¹DEPARTMENT OF GEOSCIENCES, VIRGINIA POLYTECHNIC INSTITUTE AND STATE UNIVERSITY, 4044 DERRING HALL, BLACKSBURG, VIRGINIA 24060, USA

²DEPARTMENT OF GEOLOGY, UNIVERSITY OF CINCINNATI, CINCINNATI, OHIO 45221, USA

³KENTUCKY GEOLOGICAL SURVEY, 228 MINING AND MINERAL RESOURCES BUILDING, UNIVERSITY OF KENTUCKY, LEXINGTON, KENTUCKY 40506, USA

⁴DEPARTMENT OF EARTH AND PLANETARY SCIENCE, UNIVERSITY OF CALIFORNIA, BERKELEY, CALIFORNIA 94720, USA

⁵BERKELEY GEOCHRONOLOGY CENTER, 2455 RIDGE ROAD, BERKELEY, CALIFORNIA 94709, USA

ABSTRACT

The postassembly, postrift evolution of passive margins is an essential element of global continental tectonics. Thermal and exhumational histories of passive margins are commonly attributed to a number of drivers, including uplift and erosional retreat of a rift-flank escarpment, intraplate fault reactivation, mantle-driven uplift, and erosional disequilibrium, yet in many cases, a specific factor may appear to dominate the history of a given passive margin. Here, we investigate the complex evolution of passive margins by quantifying exhumation patterns in western Scotland. We build upon the well-studied thermal evolution of the Scottish North Atlantic passive margin to test the importance of spatially heterogeneous factors in driving postorogenic burial and exhumation. Independent investigations of the cooling history from seven different field sites across the western Scottish Highlands using radiogenic apatite helium thermochronometry ((U-Th)/He; $n = 14$; ca. 31–363 Ma) and thermal modeling confirm that post-Caledonian heating and burial, as well as cooling and exhumation, must have been variable across relatively short distances (i.e., tens of kilometers). Heating associated with Paleogene hotspot activity and rifting locally explains some of this spatial variation, but additional drivers, including margin tilting during rifting, vertical separation along reactivated faults, and nonuniform glacial erosion in the late Cenozoic, are also likely required to produce the observed heterogeneity. These results indicate that passive margins may experience variable burial, uplift, and erosion patterns and histories, without exhibiting a single, dominant driver for behavior before, during, and after rifting.

LITHOSPHERE

GSA Data Repository Item 2018139

<https://doi.org/10.1130/L678.1>


INTRODUCTION

The long-term geodynamic evolution of passive margins along the cycle from collision to rifting to postrift drifting is fundamental to understanding global continental tectonics. A primary feature of the topographic, thermal, and erosional evolution observed along many passive margins is the creation and erosional retreat of a rift-flank shoulder and escarpment (e.g., Moore et al., 1986; Gallagher et al., 1994, 1995; Persano et al., 2002; Gunnell et al., 2003; Braun and Van Der Beek, 2004; Spotila et al., 2004; Persano et al., 2005; Spotila, 2005). In many locations, evidence has also recently been identified for complex uplift and erosional histories related to intraplate tectonic reactivation, dynamic uplift, and erosional disequilibrium (e.g., Roden-Tice and Tice, 2005; West et al., 2008; Prince et al., 2010; Cogné et al., 2011; Rowley et al., 2013; Amidon et al., 2016). However, the degree to which such complex histories are punctuated by tectonic and erosional events and the norm for passive-margin evolution remain unquantified. Likewise, the spatio-temporal evolution of such events along individual passive margins has yet to fully emerge due to limited data.

Low-temperature thermochronometry has served as a useful tool for quantifying the exhumation pattern and history of old orogens along rifted passive margins. Although first-order trends generally emerge for

individual passive margins, such as seaward-younging trends in apatite fission-track (AFT) and (U-Th)/He (AHe) dating (e.g., Moore et al., 1986; Gallagher et al., 1994, 1995; Gunnell et al., 2003; Spotila et al., 2004; Persano et al., 2005), dense data in specific locations often reveal punctuated histories and spatially heterogeneous patterns that depict a more complex evolution (e.g., McKeon et al., 2014; Amidon et al., 2016).

One such place is the North Atlantic passive margin of northwestern Scotland (Fig. 1), where recent thermochronologic investigations have revealed complex local histories with multiple stages of postorogenic burial and exhumation (Thomson et al., 1999; Japsen et al., 2006, 2009; Jolivet, 2007; Persano et al., 2007; Holford et al., 2009, 2010). Whether these histories are representative of the entire passive margin, or instead represent only local evolution, with as-of-yet unsampled locations possibly displaying different, but equally complex, histories, remains to be tested. This includes the possibility that some unstudied locations, including the higher-relief areas of the Scottish Highlands, may exhibit pulses of rapid late Cenozoic exhumation that may be attributable to Quaternary climate change. Some aspects of published local exhumation histories conflict with the offshore depositional record (Knott et al., 1993; Doré et al., 2002; Stoker, 2002; Evans et al., 2005; Stoker et al., 2005a, 2005b, 2005c; Anell et al., 2009) and geologic and geomorphic field relationships (Watson, 1985; Hall, 1991; Hall and Bishop, 2002). This suggests more work is required to quantify the spatio-temporal heterogeneity in

Michelle Fame  <http://orcid.org/0000-0002-0305-6910>

cooling and exhumation of this passive margin, with the ultimate goal of better understanding the role of local punctuated tectonic and geomorphic events in the geodynamic evolution of passive margins.

In this study, we refine the postcollision and postrift exhumation history of the Scottish Highlands by analyzing the thermal history of seven field sites across an ~100 km transect using AHe thermochronometry (Fig. 2). The transect runs from the coast into the interior of the Scottish Highlands (including the highest-relief areas) and crosses several important geologic and topographic features that could locally be responsible for enhancing or minimizing exhumation. Our results build on the already extensive constraints for the thermal and erosional evolution of this region and provide insight into the potential drivers of punctuated exhumation along passive margins.

BACKGROUND

Geologic Setting

The Scottish Highlands, which exhibit up to ~1 km relief, have not experienced active plate-boundary tectonic motions over the past ~50 m.y. (Fig. 1). The last mountain building event to affect Scotland was the Cambrian–Devonian Caledonian orogeny, which led to the closure of the Iapetus Ocean (McKerrow et al., 2000). Subsequent extension led to basin formation in the late Paleozoic and early Mesozoic (Doré et al., 2002; Nielsen et al., 2009), which was followed by a period of relief reduction until the Late Cretaceous, by which time the region had been reduced to low relief and experienced significant marine transgression (Hall, 1991).

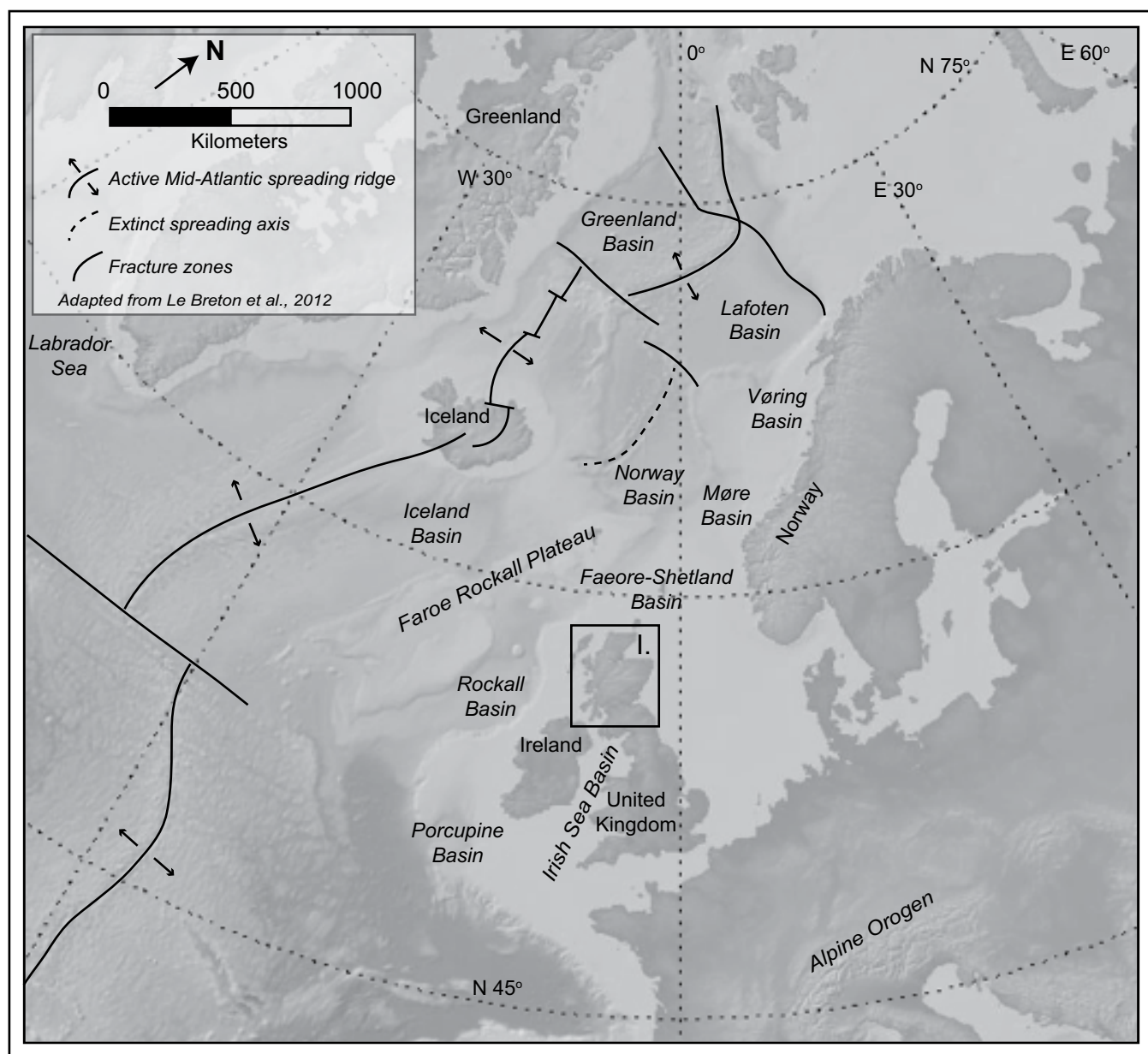


Figure 1. The North Atlantic region, adapted from Le Breton et al. (2012), showing the location of the study area (box I) and proximity to the nearest active tectonic margins, the Mid-Atlantic Ridge, the Alpine orogen, and offshore basins and features mentioned in the text. Box I shows the area covered in Figures 2 and 3. Background imagery is from the GeoMapApp.

Atlantic rifting along the northwest margin of Scotland was long-lived and volcanic in nature, peaking in the early Eocene (Doré et al., 1999). During continental breakup, western Scotland passed over the proto-Icelandic plume to produce the British Paleogene igneous complex (62–55 Ma; Anell et al., 2009; Fig. 2). Seafloor spreading continues today along the Mid-Atlantic Ridge, ~1000 km west of Scotland (Fig. 1).

The Cenozoic topographic history of the Scottish Highlands and the origin of modern relief are not fully understood. Topographic ruggedness may in part result from glacial erosion. Scotland and much of the southern part of the British Isles experienced numerous continental-scale glaciations from ca. 2.4 Ma (Shackleton and Hall, 1984; Ballantyne, 2010; Lowe and Walker, 2015) until the retreat of the last glacial event in Scotland after the termination of the Loch Lomond readvance, at ca. 11.7 ka (Fig. 2; Gollidge, 2010; Ballantyne and Stone, 2012). The influence of glaciation on modern topography is evident from the presence of “U”-shaped valleys, cirque headed tributaries, and hanging valleys (e.g., Jansen et al., 2011; Whitbread et al., 2015). However, it remains uncertain what portion of the estimated average of <1–2 km of exhumation across the Scottish Highlands since the Devonian (Watson, 1985; Hall, 1991; Hall and Bishop, 2002) can be attributed to glacial processes.

Post-Caledonian Exhumation and Burial

Low-Temperature Thermochronometry

There have been several key studies using low-temperature thermochronometry to understand the cooling history of Scotland. Persano et al. (2007) interpreted a continuous 400 m.y. cooling history with no reburial/heating events and a spike in cooling in the early Cenozoic (61–53 Ma) for Clisham and Sgorr Dhonuill in western Scotland and the Hebrides, based on AHe, AFT, and offshore depositional data (Clift et al., 1998; Fig. 2; Fig. DR1¹). They attributed the Cenozoic cooling pulse to magmatic underplating associated with emplacement of the Paleogene igneous complex. Jolivet (2007) attributed differences in Paleozoic cooling evident in AFT data at Loch Ness and Loch Linnhe to vertical movements of the Great Glen fault during a state of late Carboniferous–early Permian reactivation (Fig. 2; Fig. DR1 [see footnote 1]). No evidence for reheating/burial was found, but Jolivet (2007) did interpret a pulse of accelerated cooling at 40–20 Ma to result from ~1.6 km of rock uplift associated with far-field tectonic forces. Thomson et al. (1999) interpreted a single reheating/burial event to below 110 °C at 350–220 Ma and subsequent monotonic cooling (including ~1 km total Cenozoic exhumation), based on AFT data from the northern Scottish Highlands (Fig. 2; Fig. DR1 [see footnote 1]). AFT ages from northern Scotland in the Skye igneous complex and margins of the Minches Basin, however, imply accelerated cooling interpreted to result from Paleogene igneous activity (Thomson et al., 1999; Fig. 2).

More recent work by Holford et al. (2010) reconstructed the cooling history of Scotland’s western coast and islands (West Orkney Basin, Hebrides Sea, Isles of Skye, Mull, and Morvern), based on 79 AFT ages on basement and cover rocks, including one interior sample from near Loch Ness (Fig. 2; Fig. DR1 [see footnote 1]). Modeling of AFT ages and track-length distributions indicated cyclic post-Caledonian reheating/burial and cooling/exhumation, including major exhumation phases in the Middle

Triassic, Early Cretaceous, and Cenozoic (65–60 Ma, 45–20 Ma, and 15–10 Ma), with total Cenozoic exhumation of ~1–3 km. The exhumation history at the Isle of Morvern was particularly well constrained, due to the preservation of Pennsylvanian, Triassic, Early Jurassic, and Late Cretaceous sedimentary rocks. Holford et al. (2010) presented a complex nine-stage model of this history, which includes post-Caledonian exhumation to 350 Ma, reheating/burial to >110 °C by 250 Ma, cooling/exhumation to the surface by 200 Ma, reheating/burial to 75 °C by 130 Ma, cooling/exhumation to the surface by 65 Ma, sharp magmatic-related heating to 95 °C at 60 Ma (i.e., Paleogene igneous complex), cooling to 35 °C by 55 Ma, reheating/burial to 65 °C at 15 Ma, and late Cenozoic exhumation to the modern surface. Based on similarity between some aspects of this history and that found near the Great Glen fault (Jolivet, 2007), Holford et al. (2010) hypothesized that key elements of the complex nine-stage Morvern history apply to the broader Scottish Highlands, although this conflicts with interpretations based on other regional data (Thomson et al., 1999; Persano et al., 2007). Preferred explanations for the multiple stages of exhumation and burial are postorogenic basin formation, regional, kilometer-scale rock uplift driven by continent-ocean boundary mantle convection, and epirogenic tilting and/or intraplate compression transmitted from the Alpine orogeny and Mid-Atlantic Ridge (e.g., Knott et al., 1993; Praeg et al., 2005; Stoker et al., 2005b, 2005c; Holford et al., 2009, 2010; Stoker et al., 2010).

Offshore Record

The depositional record offshore the Atlantic coast provides additional insight into episodes of burial and exhumation of western Scotland. Four major Cenozoic unconformities in the offshore stratigraphic record are thought to result from episodes of rock uplift and exhumation.

Holford et al. (2009) integrated this record of offshore unconformities in the context of unconformities in basins traced from Norway to Ireland and AFT-based cooling histories from the British Isles and North Atlantic margin to generate a model of regional exhumation. This synthesis suggests four distinct, regionally extensive (affecting 10⁶ km²) exhumation episodes in the Early Cretaceous (120–115 Ma), early Cenozoic (65–55 Ma), mid-Cenozoic (40–25 Ma), and late Cenozoic (20–15 Ma). Holford et al. (2009) hypothesized that these regional events were produced by the proto-Icelandic plume and intraplate transmission of regional compression and associated rock uplift. This model is consistent with the cooling history interpreted for western Scotland based on AFT data by Holford et al. (2010). Green and Duddy (2010) similarly suggested that Cenozoic unconformities flanking the British Isles may be correlated across the Arctic, further suggesting that pulsed Cenozoic exhumation events spanned a broad area across the North Atlantic. If correct, the Holford et al. (2009) model of regional pulsed exhumation, which is chronicled by the cooling model for the Isle of Morvern (Holford et al., 2010), should be evident across all of the Scottish Highlands, including regions that have not previously been sampled for low-temperature thermochronometry.

Terrigenous Geologic Record

Hall and Bishop (2002) suggested that thermochronometry-derived cooling histories and the offshore sedimentary record may overestimate the magnitudes of exhumation and burial in western Scotland. Based on local observations of geomorphology, sediment provenance, reconstruction of former cover-rock extents, and depths of igneous emplacements, Hall and Bishop (2002) and earlier studies (Watson, 1985; Hall, 1991) estimated an average of <1–2 km of exhumation across the Highlands since the Devonian. For example, Hall and Bishop (2002) propose minimally denuded, “ancient” (Devonian and Mesozoic) landscapes in the

¹GSA Data Repository Item 2018139, which includes a map of apatite helium and fission track ages from prior work across the Scottish Highlands, apatite helium ages versus effective uranium for all age determinations in this study, a table showing forward model input parameters, and results and preliminary discussion of apatite ⁴He/³He thermochronometry work done for this study but which failed to produce any acceptable cooling paths, is available at <http://www.geosociety.org/datarepository/2018>, or on request from editing@geosociety.org.

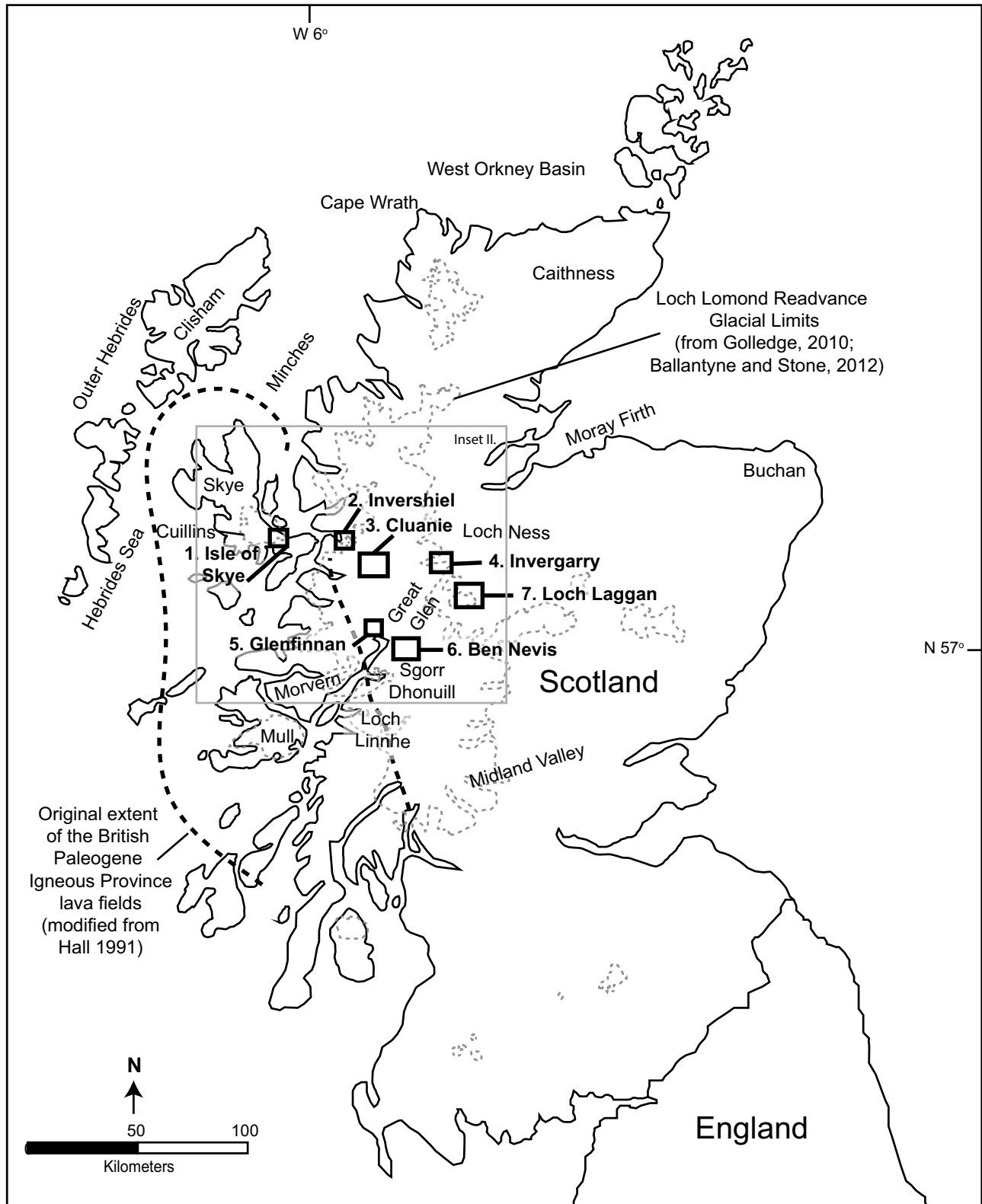


Figure 2. Study areas in Scotland mentioned in the text (adapted from Hall, 1991) and limits of the Loch Lomond readvance glacial (Golledge, 2010; Ballantyne and Stone, 2012). Inset box II represents the area in Figure 6.

Highlands and in the Lowlands of Buchan and Caithness, as well as local preservation of Devonian volcanics southeast of the Great Glen fault and near-surface intrusive rocks that lack evidence of significant burial (Fig. 2). These interpretations are inconsistent with results from earlier and subsequent AFT and AHe studies and aspects of the offshore record, however.

One inherent limitation with using offshore sediment volumes to restore exhumation is the problem of uncertainty in provenance and basin limits. For example, Scotland's Mesozoic peripheral basins may have received sediment contributions from Fennoscandia (Ziegler, 1981), as well as intrabasinal sediment recycling from submarine structural highs (Hall, 1991; Hall and Bishop, 2002). Likewise, thick Carboniferous sediment in Moray Firth, the Midland Valley, and on Morvern need not have been sourced from the Highlands, where geologic evidence implies preservation from denudation. Similarly, an inherent limitation in thermochronometry is that local data need not extrapolate across a wider region. Based on the geographic extent of quantitative thermochronometry in Scotland thus far, the onshore and offshore records of exhumation and sedimentation match (Holford et al., 2009, 2010), but this may not be the case across all areas of northwest Scotland. Reconciling this and testing the degree of heterogeneity in exhumation patterns and histories require, in part, obtaining additional thermochronometry data from the many locations not yet sampled.

METHODS

Experimental Design and Sampling Strategy

We collected 15 bedrock samples from seven field sites in a NW-SE-trending transect to test for heterogeneity in Cenozoic exhumation across the central Highlands of Northwest Scotland. The transect starts on the Isle of Skye and ends in Scotland's interior at Loch Laggan, crossing several important features that could be responsible for locally enhancing or minimizing exhumation (Figs. 2 and 3). These features include the Paleogene igneous complex, the Moine thrust, and the Great Glen fault, as well as increasing distance from the Atlantic margin to the interior of Scotland.

The western end of our sample transect consists of one low-elevation sample of a Paleogene intrusive rock from the Isle of Skye. Crossing into mainland Scotland over the Moine thrust, the second sample is a low-elevation Neoproterozoic psammite from Invershiel. While this rock was not emplaced as part of the Paleogene igneous complex, it sits close to the igneous center (Fig. 2), and the closest Paleogene-aged dike is <10 km from the sample site at Invershiel (Fig. 3). An age-elevation profile from near Loch Cluanie is next on the transect. The Cluanie site has slightly <1 km of relief and is located in the center of the Northern Highland terrane, halfway between the Moine thrust and the Great Glen fault. The next two samples are from Inverness and Glenfinnan, both of which are low-elevation samples from just northwest of the Great Glen fault (Fig. 3). The Invergarry sample was taken just south of Loch Ness, very close to the Jolivet (2007) profile, while the Glenfinnan sample was taken further south near Loch Linnhe. The sixth location consists of an age-elevation profile at Ben Nevis (Fig. 3) just southeast of the Great Glen fault. The final, furthest-inland site consists of a pair of low- and high-elevation samples taken in profile near Loch Laggan in the Grampian Highland terrane, ~20 km southeast of the trace of the Great Glen fault. Sample lithologies for all samples, including psammites and granitoids (Table 1; British Geological Survey, 2012), were chosen because they generally yield enough apatite for analysis. We analyzed the AHe-derived cooling histories of each of these seven study sites independently to see if they share common or differing post-Caledonian exhumation and burial histories.

Thermochronometry Methods

Apatite (U-Th)/He (AHe) thermochronometry is based on radiogenic production and thermally controlled diffusion of ^4He (Farley, 2000; Farley and Stockli, 2002; Ehlers and Farley, 2003). Effective closure temperature is typically 55–75 °C (Dodson, 1973; Wolf et al., 1998; Farley, 2000; Shuster et al., 2006), making it the one of the lowest thermochronological systems (Reiners and Brandon, 2006). The temperature range between ~40 °C and 85 °C is known as the partial retention zone, where ^4He is neither fully retained nor lost from the crystal (Wolf et al., 1998). Effective closure temperature is dependent on cooling rate, grain size and shape, and the amount of radiation damage that has accumulated (e.g., Dodson, 1973; Farley et al., 1996; Farley, 2000; Shuster et al., 2006; Flowers et al., 2009). The effects of varying effective closure temperatures, reheating and partial or total resetting of ages, and residence in the partial retention zone complicate resulting measured apparent AHe ages and use of the technique to determine quantitative time-temperature reconstructions.

We measured AHe ages at Virginia Tech on single and multigrain aliquots (typically ~3 grains/aliquot) from each sample. The number of aliquots analyzed per sample ranged from 4 to 13, because, in some cases, many replicates were required to yield robust mean ages. Although single-grain analyses were performed using larger (~100 μm radius) grains, generally only uniform sized grains, averaging ~60 μm radius, were used in multigrain aliquots (Table 1). We handpicked apatite at 100 \times magnification and, whenever possible, selected visibly inclusion-free grains and loaded them into Pt tubes. We outgassed the aliquots twice at 940 °C for 20 min in a resistance furnace and measured ^4He by isotope dilution using a ^3He spike and quadrupole mass spectrometer. Blank levels for ^4He detection are ~0.2 fmol, but all measured ^4He contents were much greater. We sent outgassed samples to the University of Arizona, where radiogenic parent isotopes (^{238}U , ^{235}U , ^{232}Th , and ^{147}Sm) were measured by isotope dilution and inductively coupled plasma-mass spectrometry (ICP-MS; Reiners and Nicolescu, 2006). Apatite mass was estimated using both geometrically calculated crystal volume from observed crystal shapes and assumed density, as well as direct observations of mass via ICP-MS measurement of Ca content of dissolved crystals. Average effective U ($e\text{U} = \text{U} + 0.235 \times \text{Th}$) is a parameter that essentially converts Th into U with respect to the amount of He that is produced during decay of those isotopes. Our samples average eU ranged from 4.2 to 69.6 ppm (Table 1). We applied an F_T correction to all aliquots to account for He loss due to alpha ejection prior to calculating age (Farley et al., 1996).

Apatite quality and frequency were variable among samples, corresponding to variation in AHe age reproducibility (Table 1). While clear, inclusion-free apatite was abundant in some samples, other rocks exhibited rare apatite or high occurrence of micro-inclusions and other grain flaws, including fractures, fluid inclusions, and high opacity. Samples with poor-quality apatite generally yielded less-reproducible AHe ages and required higher numbers of replicate analyses. In some cases, individual age determinations were significantly (often hundreds of millions of years) older than the bulk of replicates for a sample (Table 1). We expect these anomalously old age determinations were caused by ^4He contamination from radiogenic micro-inclusions, parent zoning, or ^4He implantation (Farley and Stockli, 2002; Shuster et al., 2006). As these anomalously old ages are not representative of sample cooling history, we removed them from the data prior to calculation of mean apparent AHe ages. We arbitrarily defined outliers as individual age determinations that were $\pm 50\%$ of the mean age (calculated iteratively; Table 1). After culling such outliers (which composed 18% of individual age determinations in the study, all of which were older than mean ages), the average standard deviation (our reported sample error) of mean AHe ages was 17% (1σ ;

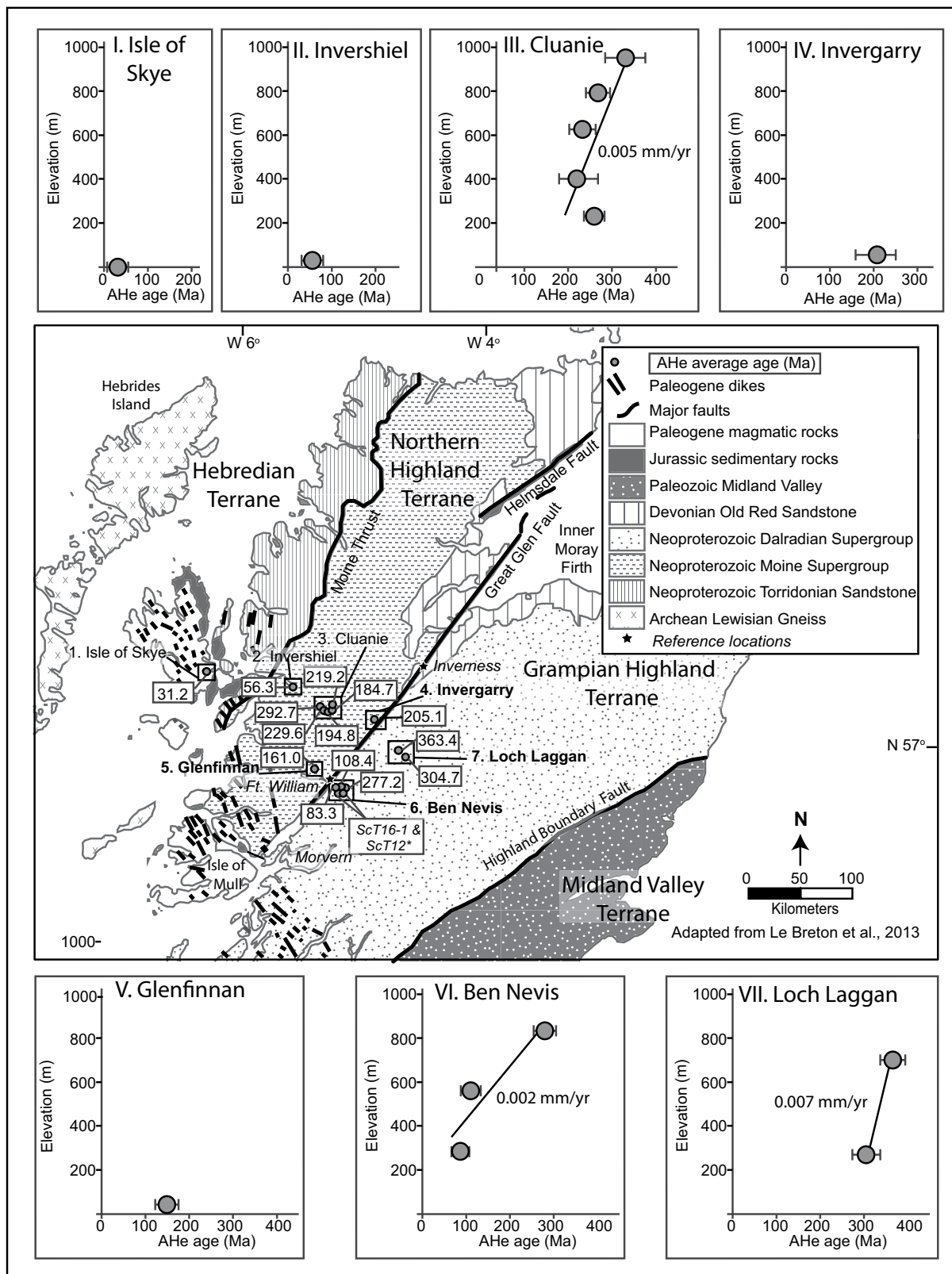


Figure 3. Major geologic terranes and bounding faults in Scotland (adapted from Le Breton et al., 2013). The seven study sites and apparent apatite (U-Th)/He (AHe) ages in Ma are represented as red points. Note locations for Ben Nevis samples ScT16-1 and ScT12, which were poorly reproduced and are not included in the analysis (see text for discussion). Graphs above and below show AHe age-elevation relationships for samples from the seven study sites. Samples from sites Cluanie, Ben Nevis, and Loch Laggan were collected in an age-elevation transects and therefore include a regression line and slope in mm yr^{-1} for the age-elevation relationship.

TABLE 1. APATITE (U-Th)/He DATA

Sample	Elev. (m)	Lat. (°N)	Long. (°W)	Rock type/ lithostratigraphic age*	Mass (µg)	mwar ¹ (µm)	He (pmol)	U (ppm)	Th (ppm)	Sm (ppm)	eU (ppm)	No. grains	F _T [§]	Corr. age	Avg. age (Ma)	Standard deviation	% culled [#]		
ScT14-02	13	57.2711	6.0635	Granite/Paleogene	0.0016	54.0	0.0013	3.0	15.3	56.77	9.5	1	0.81	26.6	31.2	Ma	5.2	20%	I. Skye
					0.0009	40.5	0.0014	5.1	22.6	1028.2	15.6	1	0.70	36.8					
					0.0013	54.0	0.0012	3.2	13.1	815.1	10.4	1	0.77	30.2					
					0.0015	27.4	0.0062	4.1	25.5	919.4	14.7	2	0.70	112.1					
ScT1	25	57.2137	5.4175	Pelite/ Neoproterozoic	0.0223	65.1	0.1332	9.2	3.8	26.7	10.2	5	0.82	136.4	56.3	Ma	17.9	38%	II. Invershiel
					0.0132	49.0	0.1009	9.3	0.5	28.2	9.6	6	0.76	199.1					
					0.0116	45.3	0.0138	5.0	0.3	21.7	5.2	5	0.74	60.1					
					0.0257	74.5	0.0521	6.5	0.6	31.7	6.8	5	0.83	69.4					
					0.0178	68.3	0.0932	8.2	1.2	28.1	8.6	6	0.82	142.0					
					0.0126	59.9	0.0506	9.5	0.9	36.2	9.9	3	0.79	98.4					
					0.0084	58.0	0.0171	8.5	0.4	36.9	8.8	3	0.79	57.0					
					0.0060	47.7	0.0602	17.4	1.5	34.6	17.9	3	0.75	141.4					
					0.0041	50.6	0.0034	6.0	1.0	21.6	6.3	1	0.76	33.7					
					0.0025	50.6	0.0017	5.8	0.3	26.0	6.0	1	0.72	30.6					
					0.0043	63.0	0.0086	5.8	0.9	22.7	6.1	1	0.80	80.4					
					0.0030	67.5	0.0036	5.8	0.6	29.9	6.1	1	0.82	47.7					
0.0030	49.5	0.0063	7.1	1.4	35.1	7.6	1	0.76	71.6										
ScT2	220	57.1469	5.1024	Psammite/ Neoproterozoic	0.0173	76.1	0.3018	20.2	0.7	139.2	21.0	4	0.82	196.1	219.2	Ma	17.9	14%	
					0.0082	51.3	0.4661	24.9	0.6	154.3	25.8	4	0.75	549.8					
					0.0077	44.6	0.1332	18.0	0.6	131.7	18.8	5	0.73	243.8					
					0.0050	57.6	0.1101	23.4	0.8	186.9	24.5	4	0.78	224.8					
					0.0068	52.4	0.1313	23.4	0.8	192.3	24.5	5	0.77	201.7					
					0.0071	54.2	0.1559	24.2	0.5	162.8	25.1	3	0.78	217.9					
					0.0049	49.1	0.2136	45.5	1.0	199.2	46.8	3	0.78	230.7					
ScT3	958	57.1210	5.1601	Pelite/ Neoproterozoic	0.0131	82.9	0.3340	21.3	5.1	123.4	23.1	3	0.86	248.0	292.7	Ma	46.0	14%	
					0.0116	72.0	0.3261	19.9	2.2	157.8	21.2	3	0.85	302.2					
					0.0144	73.7	0.4192	22.6	2.5	148.9	24.0	3	0.83	279.9					
					0.0147	113.0	0.6253	22.8	4.8	177.3	24.8	3	0.88	373.0					
					0.0123	65.9	0.5986	23.5	4.1	164.7	25.3	3	0.82	446.5					
					0.0022	55.2	0.0490	20.5	3.2	141.9	22.0	1	0.79	250.6					
					0.0090	73.6	0.2164	17.2	1.4	93.5	18.0	1	0.84	302.7					
ScT4	796	57.1188	5.1530	Psammite/ Neoproterozoic	0.0079	66.2	0.0936	12.3	0.3	64.8	12.7	4	0.81	224.1	229.6	Ma	26.9	29%	III. Cluanie
					0.0070	80.6	0.0880	14.4	0.6	41.6	14.8	2	0.84	193.6					
					0.0028	44.6	0.0433	9.8	0.6	45.8	10.2	3	0.73	392.2					
					0.0047	53.8	0.1523	14.6	1.8	61.4	15.3	3	0.79	497.2					
					0.0091	73.6	0.1668	15.2	0.4	87.4	15.8	1	0.86	260.9					
					0.0057	69.0	0.0796	12.9	0.5	30.6	13.2	1	0.81	251.2					
					0.0043	73.6	0.0390	9.0	0.2	23.2	9.2	1	0.86	218.5					
ScT5	625	57.1168	5.1474	Psammite/ Neoproterozoic	0.0095	101.2	0.0526	6.0	0.3	38.4	6.3	1	0.88	193.5	194.8	Ma	29.2	14%	
					0.0065	87.4	0.0717	5.9	0.5	38.8	6.2	1	0.88	381.9					
					0.0144	66.3	0.1127	7.0	1.3	46.6	7.5	3	0.81	248.3					
					0.0123	66.2	0.1202	10.4	4.2	62.4	11.7	3	0.81	198.6					
					0.0070	51.9	0.0375	7.0	0.6	45.4	7.3	3	0.76	184.9					
					0.0039	64.4	0.0136	4.4	0.4	29.4	4.6	1	0.79	182.2					
0.0056	87.4	0.0168	4.0	0.6	23.6	4.2	1	0.86	161.2										
ScT6	406	57.1155	5.1376	Psammite/ Neoproterozoic	0.0127	82.3	0.0494	6.9	0.3	53.1	7.3	2	0.84	124.6	184.7	Ma	42.7	43%	
					0.0051	73.2	0.1455	28.3	0.9	68.4	28.9	3	0.84	222.7					
					0.0051	58.1	0.0816	12.6	1.3	39.0	13.1	2	0.80	290.5					
					0.0009	50.6	0.0069	9.6	1.1	66.3	10.1	4	0.76	186.5					
					0.0070	74.0	0.0969	15.2	0.5	51.4	15.6	3	0.83	204.9					
					0.0108	69.0	0.7110	52.8	2.9	47.0	53.7	1	0.81	282.8					
					0.0083	78.2	0.1996	18.5	1.0	75.8	19.1	1	0.85	284.0					
					0.0144	65.2	0.4656	26.9	5.9	68.6	28.7	5	0.79	269.9					
ScT13	49	57.0927	4.7479	Granite/ Neoproterozoic	0.0290	95.8	0.4967	19.9	3.0	52.1	20.8	5	0.85	183.2	205.1	Ma	45.8	17%	IV. Invergarry
					0.0175	57.4	0.8234	49.3	9.8	70.2	51.9	5	0.77	223.1					
					0.0094	57.3	0.4956	29.3	4.8	78.5	30.8	3	0.78	410.7					
					0.0043	59.3	0.1336	34.0	7.1	110.6	36.3	2	0.81	202.5					
					0.0127	90.7	0.1454	16.7	1.8	46.0	17.4	2	0.86	147.0					

(continued)

TABLE 1. APATITE (U-Th)/He DATA (continued)

Sample	Elev. (m)	Lat. (°N)	Long. (°W)	Rock type/ lithostratigraphic age*	Mass (µg)	mwar† (µm)	He (pmol)	U (ppm)	Th (ppm)	Sm (ppm)	eU (ppm)	No. grains	F _T ‡	Corr. age	Avg. age (Ma)	Standard deviation	% culled#	
ScT16-2	16	56.8684	5.4301	Pelite/ Neoproterozoic	0.0104	73.6	0.1455	14.7	2.0	132.7	15.8	1	0.84	205.5				
					0.0088	69.0	0.0333	7.9	0.9	91.3	8.5	1	0.81	108.3				
					0.0127	82.8	0.0493	5.3	0.8	61.9	5.8	1	0.83	158.1				
					0.0100	78.2	0.0497	7.6	0.8	84.1	8.2	1	0.82	146.6	161.0	Ma	33.5	13%
					0.0200	96.6	0.1880	10.1	1.6	71.6	10.9	1	0.87	191.5	%	20.8		
					0.0101	55.7	0.0939	12.4	0.9	110.7	13.1	2	0.78	178.7				
					0.0124	73.6	0.1461	10.3	1.2	84.0	11.0	1	0.84	247.4				
					0.0100	73.6	0.0394	6.3	0.7	68.8	6.8	1	0.82	138.6				
ScT9	832	56.8003	5.0315	Granite/ Silurian–Devonian	0.0034	47.9	0.0397	6.1	20.3	664.3	14.2	3	0.74	249.0				
					0.0027	38.8	0.0635	10.1	40.5	825.3	23.7	3	0.72	295.6	277.2	Ma	24.4	0%
					0.0026	38.8	0.0429	7.5	26.2	671.0	17.0	3	0.71	299.6	%	8.8		
					0.0023	38.7	0.0380	8.0	31.1	749.1	19.0	4	0.71	264.6				
ScT10	564	56.8033	5.0412	Granite/ Silurian–Devonian	0.0041	43.3	0.0468	15.7	42.0	372.8	27.5	3	0.73	111.8				
					0.0029	36.8	0.0292	14.4	39.1	528.8	26.2	3	0.70	113.6				
					0.0097	64.8	0.2096	15.7	24.4	333.1	23.1	3	0.82	227.2				
					0.0052	55.8	0.0496	19.7	39.0	513.1	31.4	3	0.80	76.1	108.4	Ma	22.3	29%
					0.0038	42.3	0.0630	21.8	37.6	491.9	33.1	3	0.73	138.1	%	20.6		
					0.0014	46.0	0.0199	9.8	27.3	347.9	18.0	1	0.74	221.9				
0.0010	46.0	0.0118	12.0	67.2	303.6	29.3	1	0.73	102.5									
ScT11	285	56.8013	5.0551	Granite/ Silurian–Devonian	0.0054	48.2	0.0748	33.1	68.3	125.0	49.8	3	0.76	69.7				
					0.0035	42.5	0.0918	38.8	93.0	180.1	61.6	3	0.73	110.4				
					0.0043	49.2	0.1096	45.8	97.5	177.5	69.6	3	0.78	89.6	83.3	Ma	20.8	0%
					0.0042	47.4	0.0966	42.1	88.5	197.8	63.9	4	0.76	90.4	%	25.0		
					0.0045	44.8	0.0507	33.6	68.0	351.7	51.3	3	0.76	56.4				
ScT7	707	56.9597	4.5788	Psammite/ Neoproterozoic	0.0037	45.8	0.1498	28.8	2.6	166.2	30.3	3	0.74	345.0				
					0.0042	69.0	0.4795	56.5	36.9	233.5	66.4	2	0.81	403.0				
					0.0036	46.8	0.4947	43.4	49.0	214.1	56.0	3	0.73	614.7	363.4	Ma	28.4	20%
					0.0024	48.7	0.1713	47.2	15.4	219.3	51.9	3	0.72	365.1	%	7.8		
					0.0035	44.1	0.2050	42.1	5.1	203.1	44.3	3	0.73	340.6				
ScT8	268	56.9315	4.5289	Psammite/ pegmatite/ Neoproterozoic	0.0066	54.1	0.0679	7.8	2.3	50.0	8.6	3	0.78	294.6				
					0.0044	47.8	0.2047	32.9	10.5	71.0	35.8	3	0.74	328.8	304.7	Ma	31.4	0%
					0.0046	55.3	0.0855	16.3	3.2	65.4	17.3	3	0.80	255.9	%	10.3		
					0.0045	47.6	0.1324	21.0	2.9	74.9	22.0	3	0.76	333.9				
ScT12**	57	56.7705	5.0364	Granite/ Silurian–Devonian	0.0047	48.5	0.0185	120.4	22.4	149.7	126.4	3	0.77	7.8				
					0.0050	52.0	0.0257	72.3	36.6	148.3	81.6	3	0.77	15.6				
					0.0044	48.7	0.0179	65.3	79.6	84.1	84.4	2	0.79	11.8				
					0.0072	59.5	0.1384	41.6	61.2	124.8	56.6	3	0.80	80.9				
					0.0020	39.9	0.1953	25.7	53.5	315.8	39.8	3	0.72	638.1				
					0.0014	46.0	0.0004	2.6	0.7	148.4	3.5	1	0.77	24.8	14.6	Ma	6.4	58%
					0.0010	30.5	0.0094	35.5	69.7	88.8	52.3	2	0.64	52.7	%	43.7		
					0.0041	54.0	0.0352	39.2	36.7	141.4	48.5	1	0.81	42.0				
					0.0083	85.5	0.0106	1.4	1.5	155.6	2.5	1	0.85	143.4				
					0.0076	63.0	0.0174	32.2	43.1	60.3	42.7	1	0.81	12.7				
					0.0030	38.4	0.0419	19.1	33.4	328.6	28.6	2	0.72	136.8				
0.0018	31.5	0.0172	48.3	29.7	335.0	57.0	3	0.63	50.9									
ScT16-1**	44	56.7726	5.0464	Psammite/ Neoproterozoic	0.0078	69.0	0.9583	9.5	33.6	111.0	18.0	1	0.80	152.6				
					0.0067	69.0	0.1569	9.7	10.1	44.0	12.3	1	0.82	435.4				
					0.0049	46.0	0.1912	12.1	7.8	87.8	14.4	2	0.73	698.8				
					0.0284	115.0	0.5278	16.2	3.0	93.3	17.4	1	0.89	231.0	n/a	Ma	n/a	100%
					0.0071	53.4	0.0757	4.4	4.1	28.6	5.5	2	0.80	457.7	%			
					0.0159	96.6	0.0237	7.1	2.5	11.1	7.8	1	0.87	42.4				
0.0125	87.4	0.1303	8.7	1.0	80.7	9.3	1	0.88	247.7									

Note: Strikethrough individual age determinations (e.g., 0.0223) indicates anomalous ages that were not included in the average age calculation. Anomalous individual age determinations are defined as those for which ages are >50% higher than the final mean age, determined iteratively.

*British Geological Survey (2012).

†Mass weighted average grain radius.

‡F_T is the alpha ejection correction factor (Farley et al., 1996).

#Percent of anomalous aliquots divided by total aliquots.

**Ben Nevis samples SCT12 and ScT16-1 reproduced so poorly that their cooling ages were excluded from the analysis.

V. Glenfinnan

VI. Ben Nevis

VII. Loch Laggan

Ben Nevis; not reproducible**

Table 1). This dispersion in measured apparent AHe ages about the mean did not systematically correlate to grain-size variations between aliquots. The observed variance in ages was higher than the 5% (1σ) predicted cumulative uncertainty for AHe ages based on analytical precision and reproducibility of the Durango fluorapatite standard, consistent with general findings that natural samples reproduce more poorly than standards (Farley and Stockli, 2002; McDowell et al., 2005). However, it was within the range of mean 1σ error observed in recent studies at Virginia Tech, ranging from 12% (Spotila and Berger, 2010) to 22% (Tranel et al., 2011; Valentino et al., 2016), the larger of which utilized samples with similarly poor apatite quality as observed here.

Previous work has demonstrated that high parent atom concentration, or eU, can increase helium retentivity in apatite due to accumulation of radiation damage (Green et al., 2006; Shuster et al., 2006; Flowers et al., 2007). In some cases, particularly in slowly cooled terranes, this can explain high age dispersion and anomalously old AHe ages that are discrepant relative to other dating systems, such as AFT (e.g., Green and Duddy, 2006; Green et al., 2006; Flowers et al., 2007; Flowers and Kelley, 2011). This does not appear to explain the full range of dispersion in our measured ages, however, as eU does not correlate to measured age for the anomalously old ages that were culled from the data set (Fig. DR2 [footnote 1]). Measured ages that were not considered outliers did exhibit rough positive correlations with eU (Fig. DR2), however, suggesting radiation damage may have affected diffusion characteristics and produced some of the observed age dispersion. The effect of eU and He retentivity on thermal histories consistent with our measured apparent AHe ages was taken into account using the diffusion systematics of the Radiation Damage and Annealing Model (RDAAM) of Flowers et al. (2007) when modeling thermal histories using the thermal modeling program QTQt (Gallagher et al., 2005; Gallagher, 2012).

We also conducted apatite $^4\text{He}/^3\text{He}$ thermochronometry on several samples (ScT1, ScT2, ScT10, and ScT11) to better constrain the most recent cooling history of the Highlands. Apatite $^4\text{He}/^3\text{He}$ thermochronometry can more tightly constrain the continuous temperature-time ($T-t$) path of an individual apatite as it cooled through the partial retention zone than AHe ages alone by matching modeled cooling paths to the measured diffusion profile of ^4He across an apatite (Shuster and Farley, 2004, 2005; see supplement 4 for a full discussion [footnote 1]). The diffusion profiles for samples ScT1, ScT10, and ScT11 failed to produce any acceptable cooling paths (Fig. DR3 [footnote 1]). While we do not know the exact reason why these samples failed, there are different analytical possibilities, including a spatially nonuniform distribution of parent U and Th, ^4He -rich inclusions, or other as-yet-unknown systematics that can significantly influence the distribution of ^4He throughout a crystal, affecting the final form of the diffusion distribution (Shuster and Farley, 2004, 2005). As such we cannot use the data for ScT1, ScT10, and ScT11. The diffusion profile for ScT2 did produce acceptable cooling paths when we removed the outer portion of the diffusion profile that plotted outside of end-member envelopes, indicating a uniform initial distribution of ^4He (Shuster and Farley, 2004, 2005; see also Fig. DR3 [footnote 1]). Again, this indicates the possibility for analytical factors to have affected the final form of the diffusion distribution, in this case, possibly a ^4He -rich inclusion near the grain edge (Shuster and Farley, 2004, 2005). Since we did not measure U and Th distributions within any of the sampled crystals prior to dissolution for parent isotope measurement, we are unable to assume parent nuclide distributions or determine the actual cause of the failure of the diffusion profiles to produce acceptable cooling paths. Apatite $^4\text{He}/^3\text{He}$ data and a full discussion of preliminary analysis for samples ScT1, ScT2, ScT10, and ScT11 can be found in supplement 4, Table DR2, and Figure DR3 (footnote 1).

The possibility of zonation of parent isotopes in samples analyzed for $^4\text{He}/^3\text{He}$ calls into question whether apatite analyzed for AHe ages may have been zoned. The alpha ejection correction method (F_T correction; Farley et al., 1996) assumes a uniform distribution of ^4He , but zoned apatite may eject more or less ^4He than uniform apatite. Trace-element zonation was not apparent in apatite from sample ScT12 based on scanning electron microscopy cathodoluminescence imaging, but zonation was not otherwise investigated. This leaves open the possibility that some samples were affected by parent isotope zonation, which may have contributed to the observed age dispersion.

Time-Temperature Modeling Based on Measured Ages

We used the thermal modeling program QTQt (Gallagher et al., 2005; Gallagher, 2012) to carry out both forward and inverse modeling to assist in interpretation of the samples' $T-t$ histories. We chose to use QTQt because it allows for the input of multiple samples in a vertical profile to derive a single cooling history. Our samples approximate a vertical profile and were collected at various elevations at the surface from peaks down to valleys (e.g., Huntington et al., 2007). To account for the effects of radiation damage in our samples, we used the diffusion systematics of RDAAM from Flowers et al. (2007) in all model runs. While the modern geothermal gradient in Scotland is $25.3\text{ }^\circ\text{C km}^{-1}$ (Holford et al., 2010), paleogeothermal gradients across Scotland may have been as high as $60\text{ }^\circ\text{C km}^{-1}$ during times of higher heat flow, such as in the early Cenozoic and Carboniferous (e.g., Thomson et al., 1999; Persano et al., 2007; Holford et al., 2010). Therefore, following Thomson et al. (1999), we used a typical geothermal gradient of $30\text{ }^\circ\text{C km}^{-1}$ for models, but we addressed the impacts of a possibly changing geothermal gradient. We input the modern-day surface temperature as $10\text{ }^\circ\text{C}$ for all models based on an average of recorded temperatures from the UK Met-Office (2013). For the three age-elevation profiles, we offset the temperature of the lowest-elevation sample below the highest-elevation sample based on their elevation difference and the $30\text{ }^\circ\text{C km}^{-1}$ gradient, resulting in a temperature offset of $22\text{ }^\circ\text{C}$ at Cluanie, $24\text{ }^\circ\text{C}$ at Ben Nevis, and $13\text{ }^\circ\text{C}$ at Loch Laggan. During inverse modeling, we allowed temperature offset to vary throughout $T-t$ history. At $t = 0$ Ma, we prescribed there to be no offset in temperature between high- and low-elevation samples, because low relief and typical lapse rate imply only a slight difference in ambient surface temperature.

QTQt forward modeling allows for calculation of expected AHe ages based on the input of defined cooling paths for samples. We used forward modeling in QTQt to determine if all, or only some, of the burial and exhumation cycles at Morvern from Holford et al. (2010) were compatible with our measured AHe ages. For the three sample areas with age-elevation profiles, the thermal histories shown are for the highest-elevation samples (Fig. 4). The first input thermal history, forward model 1 (FM-1), included the entire nine-step thermal history of Morvern from Holford et al. (2010; see also Fig. 4; Table DR1). Seven other models were run that incrementally simplified the initial model, by removing the most recent step in the cooling history. For example, thermal history FM-2 skips the late Cenozoic heating and burial to $65\text{ }^\circ\text{C}$ at 15 Ma. The simplest model, FM-8, involves monotonic cooling to the surface from a starting point of $35\text{ }^\circ\text{C}$ at 350 Ma (Fig. 4; Table DR1). The sample from the Isle of Skye is itself a Paleogene igneous complex plutonic rock (British Geological Survey, 2012). Therefore, for the Isle of Skye, only models FM-1 and FM-2, the only two models impacted by Paleogene igneous heating, were tested, and all heating and cooling events occurring prior to the Paleogene were removed (Fig. 4). The reasoning behind eliminating steps in this manner was to determine the level of complexity in the cooling history required by the AHe data. The simpler cooling histories resembled those

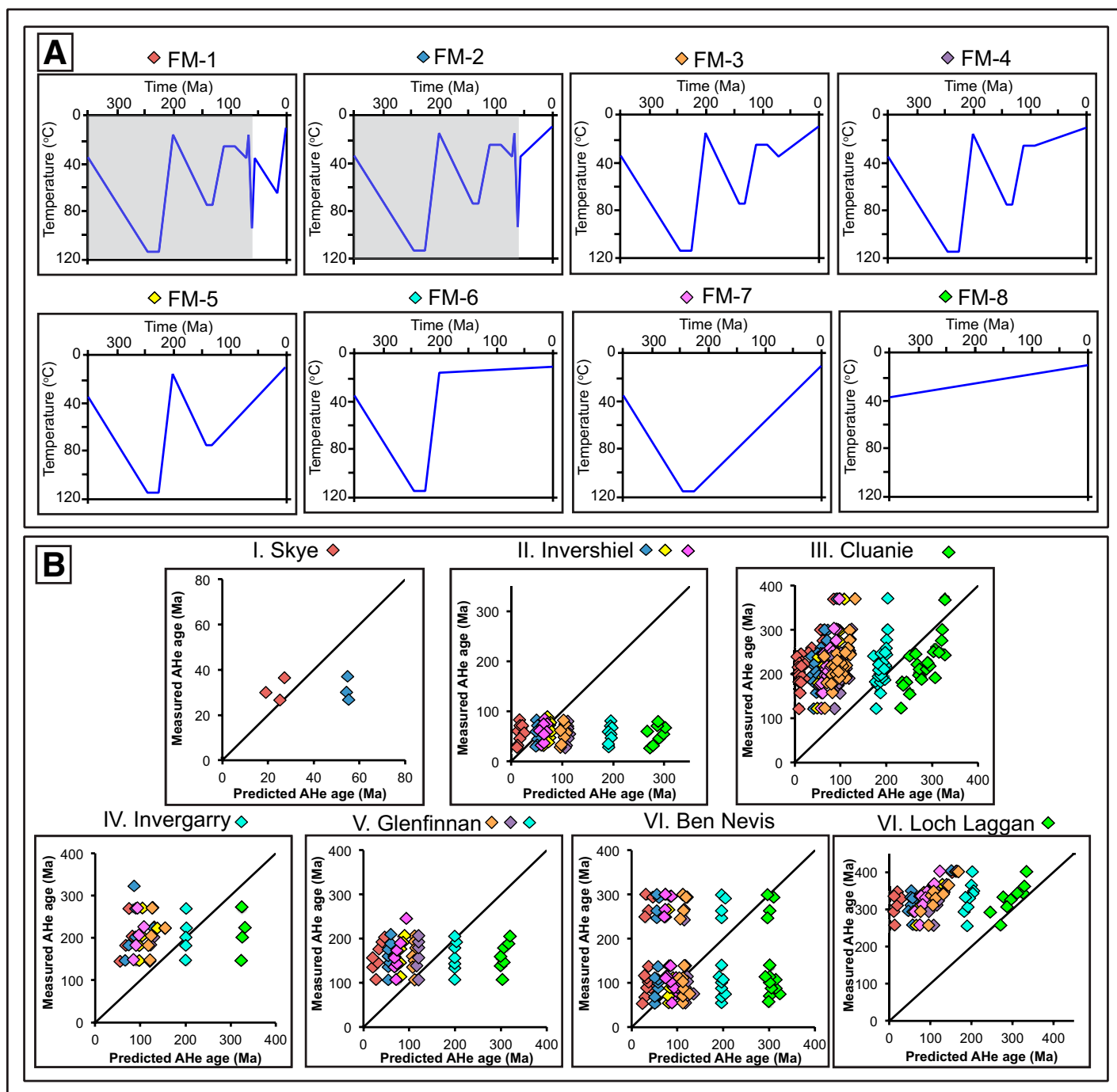


Figure 4. Summary of thermochronology modeling and predicted apatite (U-Th)/He (AHe) ages. (A) Input temperature-time ($T-t$) paths used in QtQT forward modeling (FM) adapted from (Holford et al., 2010). For specific input forward $T-t$ points for each path, see Table DR1 (text footnote 1). (B) Graphs of measured individual age determinations vs. model-predicted age determinations from forward models that display how well each $T-t$ path predicts the observed age determinations. Colored diamonds on the graphs represent the input $T-t$ path, with the same colored diamond beside the title of each path in A. Colored diamonds next to each field area name represent those input forward model considered a best fit for that location (see full discussion in the text). Since the sample from the Isle of Skye is itself a Paleogene igneous complex plutonic rock (British Geological Survey, 2012), only models FM-1 and FM-2 were tested (the only two models impacted by Paleogene igneous heating), and all heating and cooling events occurring prior to the Paleogene were removed, as indicated by heating and cooling events under the gray boxes in FM-1 and FM-2.

suggested in other studies (e.g., Thomson et al., 1999; Hall and Bishop, 2002; Persano et al., 2007). We used plots of all individual AHe age determinations predicted from the models versus observed individual AHe age determinations for each sample aliquot to illustrate the best-fit model (Fig. 4). Specific $T-t$ inputs for all models are provided in Table DR1 (footnote 1).

We also ran inverse models using QTQt for the three locations with age-elevation profiles (Cluanie, Ben Nevis, and Loch Laggan). For each model run, the only $T-t$ point we constrained was the initiation point at 35 °C at 350 Ma (Holford et al., 2010), indicating exhumation of basement rock nearly to the surface following the end of the Caledonian orogeny. Extensive exhumation of the Caledonian Mountains by 350 Ma is also consistent with observations of Watson (1985) and Hall and Bishop (2002), which suggest Devonian unroofing of the post-Caledonian Newer Granites by the end Devonian. All models allowed the offset temperature between the highest- and lowest-elevation samples to vary through time; this allowed the production and destruction of relief to influence the cooling paths. For each inverse model, we ran 150,000 model iterations and allowed burial to influence the output $T-t$ path. We report both “maximum likelihood” and the preferred “expected” model outcomes (Fig. 5; Gallagher et al., 2005). The maximum likelihood models attempt to best predict the output age with no regard for model complexity (i.e., the number of $T-t$ nodes in the output thermal history), while the expected model best fits the data while minimizing complexity of the predicted thermal history.

RESULTS

Thermochronometry Results

Average apparent AHe ages from the study range from 31.2 ± 5.2 Ma to 363.4 ± 31.4 Ma (Table 1; Fig. 3). The three ages from the Ben Nevis profile range from 83.3 ± 20.8 Ma to 277.2 ± 24.4 Ma, the five ages from the Cluanie profile range from 184.7 ± 42.7 Ma to 292.7 ± 46.0 Ma, and the two ages from Loch Laggan profile range from 304.7 ± 31.4 Ma to 363.4 ± 28.4 Ma (Fig. 3; Table 1). Within error, all sample ages in age-elevation profiles increased with a positive, linear trend with elevation (Fig. 3). The single ages from the other regions are 56.3 ± 17.9 Ma at Invershiel, 205.1 ± 45.8 Ma at Invergarry, 31.2 ± 5.2 Ma at the Isle of Skye, and 161.0 ± 33.5 Ma at Glenfinnan (Table 1; Fig. 3).

Several samples exhibited extreme age dispersion and could not be interpreted, despite their potential importance for constraining the cooling history of the region. One such sample, ScT12, a granitic, low-elevation (57 m above mean sea level [amsl]) sample from the Ben Nevis profile, had an average AHe age of 14.6 Ma (Table 1). Such a young age could have significant implications on Scottish Cenozoic exhumation and burial, if correct. However, ScT12 reproduced very poorly, with 58% anomalous aliquots (of $n = 12$; Table 1), and therefore we do not trust the age to be accurate or interpretable. Due to the possible importance of such a young age, we resampled another low-elevation sample, ScT16-1 (44 m amsl; Table 1) from a different lithology (psammite) at the same location, but this had no reproducible age determinations and also had to be excluded from interpretations (Table 1). Why samples from two different lithologies in this location failed to yield reproducible ages is unclear. The fact that a low-elevation sample from near Ben Nevis could record Neogene cooling should be viewed as a lingering possibility.

The age-elevation profiles yielded gradients that are typically associated with slow time-averaged exhumation or prolonged stasis in the He partial retention zone. The slope of all three age-elevation profiles predicts a slow average exhumation rate of <0.01 mm/yr applicable to the Permian to Early Jurassic at Cluanie, the Permian to Late Cretaceous at

Ben Nevis, and in the Carboniferous at Loch Laggan (Fig. 3). The degree to which observed age-elevation gradients represent the actual exhumation rates during those periods, as opposed to prolonged durations in the partial retention zone or reheating and partial resetting, is best addressed via results of our modeling of thermal histories based on measured AHe ages (see following section).

Results of the $^4\text{He}/^3\text{He}$ analysis failed to produce acceptable $T-t$ trajectories for samples ScT1, ScT11, and ScT12 (see supplement 4, Fig. DR3 [footnote 1]). Acceptable fit cooling trajectories for ScT2 $^4\text{He}/^3\text{He}$ analysis should be viewed with uncertainty, because the outer portion of the diffusion profile that plotted outside of the uniform initial distribution of ^4He end-member envelope was removed prior to analysis. Acceptable cooling paths for ScT2 hint at the possibility for renewed exhumation in the Cretaceous through the Cenozoic at the Cluanie field site, following a period Carboniferous to Permian exhumation stagnation (see supplement 4, Fig. DR3 [footnote 1]).

Forward Modeling

Forward models of thermal histories based on measured AHe ages indicate that a single common $T-t$ history cannot account for the measured ages across the seven sample sites. Best-fit forward models for the four single-sample sites (Skye, Invershiel, Glenfinnan, and Invergarry) were chosen because those were the models for which the measured versus model-predicted age determinations intersected the 1:1 best-fit line (Fig. 4). The best-fit forward model for the Isle of Skye was FM-1, or the complete thermal history of Morvern from Holford et al. (2010) with all pre-Paleogene aged events removed. In this model, apatite cooled quickly following Paleogene igneous crystallization, was subsequently heated in the Cenozoic to 65 °C at 15 Ma, presumably from burial, and was then exhumed to the surface (Fig. 4). The best-fit forward models for Invershiel were FM-2, FM-5, and FM-7 (Fig. 4), although FM-2 may be most likely given the proximity to the Paleogene igneous province (Fig. 3). The only elements missing from FM-2 relative to FM-1 are Neogene burial and reheating. Glenfinnan’s best-fit models included FM-3, FM-4, and FM-6, all of which involve heating in the late Carboniferous and cooling by the Early Jurassic. Models FM-3 and FM-4 included reheating in the Late Jurassic. Invergarry’s best fit was model is FM-6 (described above; Fig. 4).

For the three sample sites with age-elevation profiles (Cluanie, Ben Nevis, and Loch Laggan), the best-fit forward models were not those where the measured versus model-predicted age determinations simply intersected the 1:1 best-fit line. Rather, a best fit for these sample sites required the measured age-elevation relationship to be recreated by the model predicted ages (i.e., the measured vs. predicted ages needed to lie along the 1:1 best-fit line’s slope rather than simply intersect it; Fig. 4). For example, in the Cluanie forward models, FM-6 did predict some individual age determinations well, but model FM-8 (monotonic cooling from the starting point) was a much better fit for Cluanie’s age-elevation relationship (Fig. 4). FM-8 was also the best-fit inverse model for Loch Laggan. For Ben Nevis, no single model fit both the older higher-elevation age determinations and the lower-elevation younger age determinations. Thus, it was not possible to define a best-fit forward model for Ben Nevis via this set of forward models, but we can exclude model FM-1, because it underpredicted all Ben Nevis age determinations.

Inverse Modeling

One of the motivations for inverse modeling in the three profile locations (Cluanie, Ben Nevis and Loch Laggan) was the poor performance of the forward models in predicting the age-elevation relationships that we

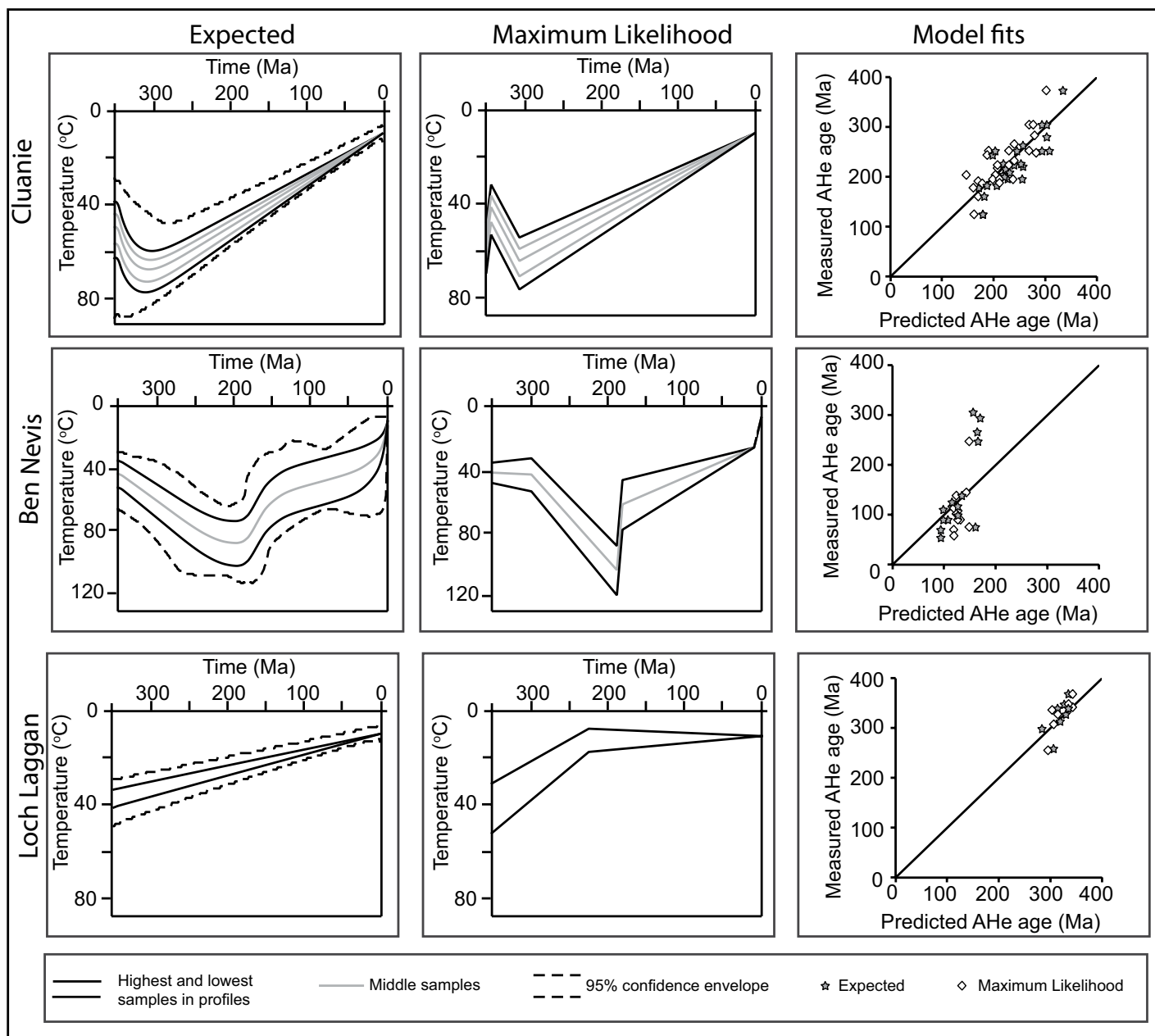


Figure 5. Results of QTQt inverse modeling for the three field areas with age-elevation data, including Cluanie (top row), Ben Nevis (middle row), and Loch Laggan (bottom row). The first column shows the expected modeled $T-t$ path with 95% confidence envelopes. The second column shows the results of the modeled maximum likelihood $T-t$ path. The third column shows model-predicted vs. measured age determinations for the expected (gray stars) and maximum likelihood (white diamonds) inverse models. The line in each graph is a 1:1 best-fit line, representing where the points would plot if the predicted age determinations perfectly matched the measured age determination. AHe—apatite (U-Th)/He.

observed. Based on inconsistencies with existing models, it was necessary to use inverse modeling to explore new cooling histories (Fig. 5). We report both “maximum likelihood” (the $T-t$ history that best predicted the measured age determinations with no regard for model complexity) and the preferred “expected” (the $T-t$ history that best fit the data while minimizing complexity) model outcomes (Fig. 5; Gallagher et al., 2005). Inverse modeling of the Cluanie profile output $T-t$ histories that predicted slight burial and reheating by the end Carboniferous, followed by continuous slow cooling to the surface. Inverse modeling of the Loch Laggan profile output $T-t$ histories indicating slow monotonic cooling of both samples from the starting point to the surface without any reheating (Fig. 5). At Ben Nevis, inverse modeling predicted one stage of heating starting in the early Carboniferous and reaching highest temperatures in the Early Jurassic, followed by a short pulse of relatively quick cooling (Fig. 5). Subsequently, the samples experienced monotonic, but differential cooling between highest -and lowest-elevation samples to the surface. Inverse model results at Cluanie and Loch Laggan did a good job at predicting the age-elevation relationships that we observed (Fig. 5). However, at Ben Nevis, the highest-elevation measured age determinations were still under-predicted by the inverse model-predicted age determinations (Fig. 5), and it was still not possible to define a best-fit $T-t$ model for Ben Nevis.

DISCUSSION

Comparison of Apparent AHe Ages to Previous Work

All apparent AHe ages are younger than their lithostratigraphic age (British Geological Survey, 2012), and most are consistent with the range of previous AFT and AHe ages taken from Scotland, which range from ca. 300 Ma to ca. 50 (Thomson et al., 1999; Jolivet, 2007; Persano et al., 2007; Holford et al., 2010; Fig. DR1). There were several exceptions, however. Despite the lower closure temperature of AHe thermochronometry, both samples from the Loch Laggan profile (ScT7 and ScT8; ca. 305 and ca. 364 Ma, respectively) were older than previously reported AFT ages from the Scottish Highlands (Fig. 3; Fig. DR1). These apparent AHe ages were not taken from the same locations as the younger AFT ages, so it is feasible that these disparities result from spatially heterogeneous thermal histories across Scotland. These oldest apparent AHe ages, as well as ages from the highest samples at Cluanie and Ben Nevis (ScT3 and ScT9; ca. 280 and ca. 290 Ma, respectively), were also older than the oldest low-temperature thermochronology ages measured from other passive-margin mountain ranges, including the Appalachians of North America (e.g., Spotila et al., 2004; Roden-Tice and Tice, 2005; Taylor and Fitzgerald, 2011; McKeon et al., 2014) and other margins worldwide (e.g., Gallagher and Brown, 1999). The oldest AHe ages in Scotland are instead reminiscent of the oldest low-temperature thermochronology ages found in the continental interiors that lie hundreds of kilometers into the hinterland of other passive margins worldwide (Gallagher and Brown, 1999), such as in the Canadian Shield, where AHe ages range up to 650 Ma (Flowers et al., 2009). Our data may support the idea that the interior of Scotland was preserved from deep exhumation for hundreds of millions of years, such that the remaining mountain peaks once persisted as part of a stable landscape before being elevated and incised in the Cenozoic (George, 1966; Hall, 1991). There is also the possibility that these ages are erroneously old due to undocumented effects of radiation damage or other factors on He diffusion in very old crystals (e.g., Green et al., 2006). The general agreement with other thermochronometers and geologic observations, however, suggests this is unlikely to be the case. As such, we choose to interpret the mean apparent AHe ages as determined, although excluding statistical outliers for each sample.

Heterogeneous Post-Caledonian Cooling Histories

Spatially heterogeneous post-Caledonian heating and cooling are necessary to produce the measured apparent AHe ages at our seven field sites, consistent with previous interpretations of low-temperature thermochronometry in northwest Scotland (e.g., Thomson et al., 1999; Holford et al., 2010). The addition of these new data permit refinement of the degree of spatial and temporal heterogeneity in postorogenic evolution of the passive margin, which aids in understanding potential geodynamic drivers.

Several distinct periods of post-Caledonian heating and cooling found in previous studies (e.g., Thomson et al., 1999; Jolivet, 2007; Persano et al., 2007; Holford et al., 2009, 2010) are compatible with the measured apparent AHe ages from some, but not all, of our seven field areas based on forward and inverse QTQt modeling (Fig. 6; Table 2). Proposed possible heating and cooling histories consistent with the measured apparent AHe ages at our seven study areas are displayed in Figure 6. Multiple possible paths are displayed for some study areas where multiple cooling histories were able to produce our measured apparent AHe ages. Major heating events followed by cooling occurred in (1) the late Paleozoic to early Mesozoic, (2) the Late Jurassic to Early Cretaceous, (3) the Late Cretaceous, (4) the Paleogene, and (5) the Neogene.

Late Paleozoic to early Mesozoic heating and cooling events (events B through C in Table 2; Fig. 6) were contemporaneous with post-Caledonian extension and the creation of intraplate late Paleozoic and early Mesozoic sedimentary basins that are thought to have buried most of the Scottish Highlands (e.g., Hall, 1991; Thomson et al., 1999; Doré et al., 2002; Nielsen et al., 2009; Holford et al., 2010). Remnants of this burial event are kilometer-scale Carboniferous sedimentary sections preserved in Moray Firth, the Midland Valley, and on Morvern (Watson, 1985; Hall, 1991; Hall and Bishop, 2002). The Great Glen fault was likely reactivated as a strike-slip fault during the Permian as a result of basin inversion in the Orkney area (Jolivet, 2007). This period of burial is compatible with all best-fit forward model iterations at Invershiel, Invergarry, and Glenfinnan, the Cluanie inverse model, and possibly with the poorly fitting Ben Nevis inverse model (Fig. 6; but not the Cluanie best-fit forward models). This suggests that all of those areas may have been buried in the late Paleozoic to early Mesozoic. A deep burial event is not compatible with any model iterations at Loch Laggan, where instead model results suggest slow, steady exhumation (<0.01 mm/yr) during the Carboniferous, similar to the age-elevation profile (Fig. 3). However, we cannot completely exclude the possibility of shallow burial to temperatures below ~40 °C at Loch Laggan. The late Paleozoic to early Mesozoic burial event is also not applicable to the Isle of Skye, given that the rocks sampled there have younger crystallization ages (Paleogene).

The Late Jurassic to Early Cretaceous heating and cooling events (events D–E in Table 2; Fig. 6) have been attributed to contemporaneous basin formation in Scotland and burial of the highlands, resulting in the formation of the Jurassic sedimentary rocks that currently outcrop along Scotland’s coast (Fig. 3; Holford et al., 2010). This period of burial and subsequent exhumation is compatible with some, but not all, best-fit forward model iterations at Invershiel and Glenfinnan. The event is not compatible with any model iterations, forward or inverse, at Cluanie, Invergarry, Ben Nevis, or Loch Laggan, and it is not applicable to the Isle of Skye due to the sampled rock’s Paleogene crystallization age. Late Cretaceous burial and exhumation (events F–G in Table 2; Fig. 6), attributed to Late Cretaceous marine transgression and chalk deposition (Hall, 1991; Hall and Bishop, 2002; Holford et al., 2010), are also compatible with some, but not all, best-fit forward model iterations at Invershiel and Glenfinnan.

Paleogene heating and cooling (events H through I in Table 2; Fig. 6) are considered largely to have been magmatic, rather than a result of burial,

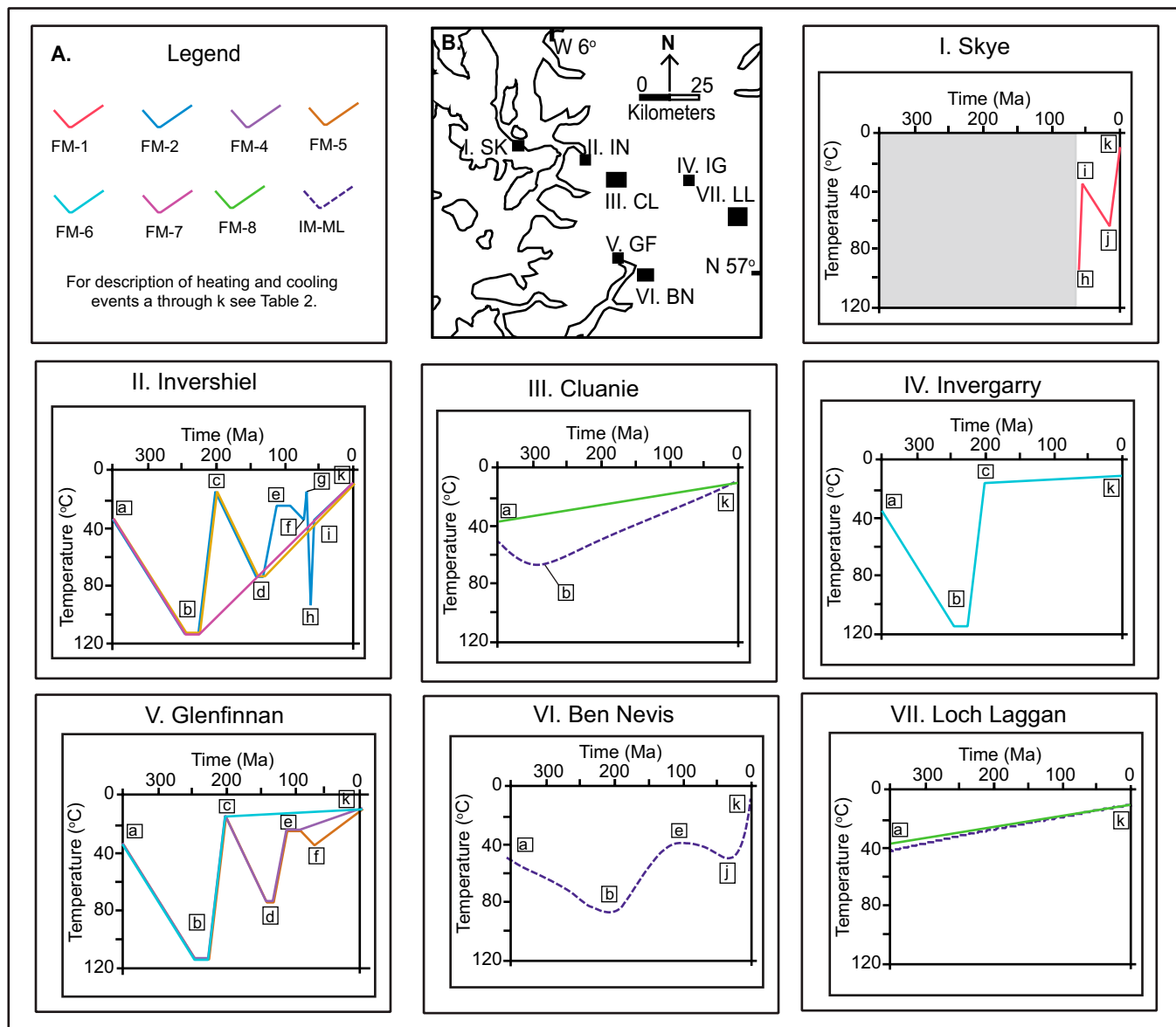


Figure 6. (A) Solid colored lines in boxes I–VII refer to cooling paths derived from forward models (FM) 1 through 8 from Figure 4, and dashed line refers to inverse model maximum likelihood cooling paths (IM-ML) from Figure 5. Descriptions and citations for evidence of heating and cooling events a through k in boxes I–VII are summarized in Table 2. (B) Map area is from inset II in Figure 2, showing the seven field areas in this study (displayed as black boxes): I—SK (Skye), II—IN (Invershiel), III—CL (Cluanie), IV—IG (Invergarry), V—GF (Glenfinnan), VI—BN (Ben Nevis), and VII—LL (Loch Lomond). Boxes I through VII display our proposed possible heating and cooling histories consistent with measured apparent apatite (U-Th)/He (AHe) ages at our seven study areas. Multiple possible paths are displayed for single study areas where multiple cooling histories are able to produce the measured apparent AHe ages. The cooling histories on the Isle of Skye apply only to the Cenozoic, because the sample is a Paleogene-aged igneous rock (gray box indicates the pre-Paleogene).

TABLE 2. SUMMARY OF HEATING AND COOLING EVENTS

Event*	Timing and event type	Description†
k	Present day	Cooled to the surface (1, 2)
j	Late Cenozoic heating and cooling	Burial by late Cenozoic sediments; uplift and erosion from far-field tectonic forces and glacial exhumation; late Cenozoic offshore unconformity and Neogene margin escarpment (1, 3, 4, 5, 6)
i	Paleogene cooling	Post-igneous event cooling; uplift and exhumation from underplating and Alpine orogenesis; early and mid-Cenozoic offshore unconformities (1, 4, 7, 8, 9, 10, 11, 12)
h	Paleogene heating	Magmatic heating from North Atlantic rifting and Paleogene igneous complex emplacement (1, 9, 13); formation of Skye Paleogene aged plutonic rock (14)
g	Late Cretaceous cooling	Pre-Paleogene magmatic complex exhumation (1)
f	Late Cretaceous heating	Marine transgression resulting in burial and Cretaceous chalk deposition (1, 9, 13)
e	Early Cretaceous cooling	Exhumation resulting in the formation of the Early Cretaceous offshore unconformity (1, 4)
d	Jurassic to Early Cretaceous heating	Basin formation burial; deposition of Jurassic sedimentary rocks presently along Scotland's coast (1, 15)
c	Triassic cooling	Exhumation of Mesozoic cover rocks (1)
b	Late Paleozoic to early Mesozoic heating	Burial during postorogenic extension creating intraplate sedimentary basins; deposition of Carboniferous sedimentary sections preserved on Moray Firth, the Midland Valley, and on Morvern; Permian reactivation of the Great Glen fault and basin inversion in Orkney (1, 5, 9, 11, 13, 16, 17, 18)
a	End Devonian cooling	Postorogenic exhumation and unroofing of Strontian volcanics and post-Caledonian Newer Granites (1, 9, 18)

*Events a through k displayed are in Figure 6.

†Descriptions of heating and cooling events are summarized from the following sources: 1—Holford et al. (2010), 2—Met-Office U.K. (2013), 3—Whitbread et al. (2015), 4—Holford et al. (2009), 5—Jolivet (2007), 6—Praeg et al. (2005), 7—Persano et al. (2007), 8—Anell et al. (2009), 9—Hall and Bishop (2002), 10—Stoker (2002), 11—Thomson et al. (1999), 12—Clift et al. (1998), 13—Hall (1991), 14—British Geological Survey (2012), 15—Le Breton et al. (2013), 16—Nielsen et al. (2009), 17—Doré et al. (2002), and 18—Watson (1985).

and were associated with the emplacement of the Paleogene igneous complex (e.g., Hall, 1991; Hall and Bishop, 2002; Persano et al., 2007; Holford et al., 2010). This event corresponds to an offshore Paleocene unconformity (ca. 62–55 Ma; e.g., Stoker, 2002; Anell et al., 2009). Rapid cooling after the magmatic event has been attributed to localized uplift due to underplating or exhumation driven by dynamic topographic uplift (Persano et al., 2007; Holford et al., 2010; Cogné et al., 2016). Paleogene cooling has also been explained by enhanced uplift and exhumation associated with the far-field compressional effects of Atlantic rifting and Alpine orogenesis causing upper-crustal folding and fault reactivation in Scotland (e.g., Jolivet, 2007; Holford et al., 2010; Stoker et al., 2010; Cogné et al., 2016). Paleogene heating and cooling are compatible with all best-fit forward model iterations on the Isle of Skye and are compatible with some best-fit forward model iterations at Invershiel. The Isle of Skye and Invershiel are both located near the original extent of Paleogene magmatism (Fig. 2). Paleogene heating is incompatible with all model iterations at Cluanie, Invergarry, Glenfinnan, and Loch Laggan, suggesting that Paleogene heating was localized (Fig. 6).

The Neogene event (event J in Table 2; Fig. 6) is thought to have been associated with burial followed by uplift and exhumation due to intraplate compression (e.g., Jolivet, 2007; Holford et al., 2010; Stoker et al., 2010). This event corresponds with the offshore base-Neogene unconformity (e.g., Stoker, 2002; Anell et al., 2009). The Neogene event is compatible with all model iterations on the Isle of Skye and possibly with the poorly fitting Ben Nevis inverse model, but it is not compatible with any model iterations in the other field areas, suggesting that this event was localized (Fig. 6). Enhanced Neogene exhumation on the Isle of Skye may have resulted from differential uplift of the region via warping of Scotland's Atlantic margin by intraplate compression, which created a Paleogene–Neogene scarp between the Cuillins on the Isle of Skye and Cape Wrath (Hall and Bishop, 2002; see also Fig. 2).

No best-fit forward or inverse model iterations that predict the measured Loch Laggan apparent AHe ages are consistent with post-Caledonian heating events to temperatures greater than 40 °C (Figs. 4, 5, and 6). This suggests that the Loch Laggan region has not experienced significant

burial after 350 Ma, and instead has been slowly exhuming or experiencing crustal stasis. Hall and Bishop (2002) suggested that it is likely that parts of the Highlands have been above sea level and never buried since the end-Caledonian, as sources of sediment rather than basins, and the Loch Laggan site may be one of those locations. The location is in the center of the Grampian Highland terrane, far away from both the Great Glen fault to the northwest and the Highland Boundary fault to the southeast (Fig. 3). The region may have remained a high point, and possibly sediment source, during periods of intracontinental basin formation and burial. It is also far enough inland to not have been significantly impacted by Atlantic margin tilting during rifting (e.g., Praeg et al., 2005). The morphology of the Loch Laggan region hosts a high plateau, known as Creag Meagaidh, which is very different than the highly dissected morphology of the rest of the Scottish Highlands, and perhaps can be attributed to the region's long-term stability.

The different *T-t* paths required to fit measured apparent AHe ages across our field sites (Fig. 6), all within ~20–100 km of each other, suggest that different burial, magmatic, and tectonic histories can occur across very short distances, even during the postorogenic evolution of ancient mountain ranges along present-day passive margins. The distances over which these differences are manifest are short, particularly considering that the typical wavelength of exhumational responses to crustal loading and unloading in lithosphere with a typical flexural rigidity is typically several hundred kilometers (Montgomery, 1994). This suggests some of the differential cooling and burial-exhumation between these sites was driven tectonically (possibly accommodated by local faulting both during basin formation and during exhumation), but was not isostatically compensated.

Cenozoic Exhumation

Total Cenozoic exhumation depths across the study area range from 0.2 to 1.8 km, with larger estimates at the Isle of Skye and Ben Nevis and lower estimates for Loch Laggan and Invergarry (Fig. 7). These estimates were calculated based on the maximum Cenozoic temperature in the best-fit models for each sample site, a surface temperature of 10 °C,

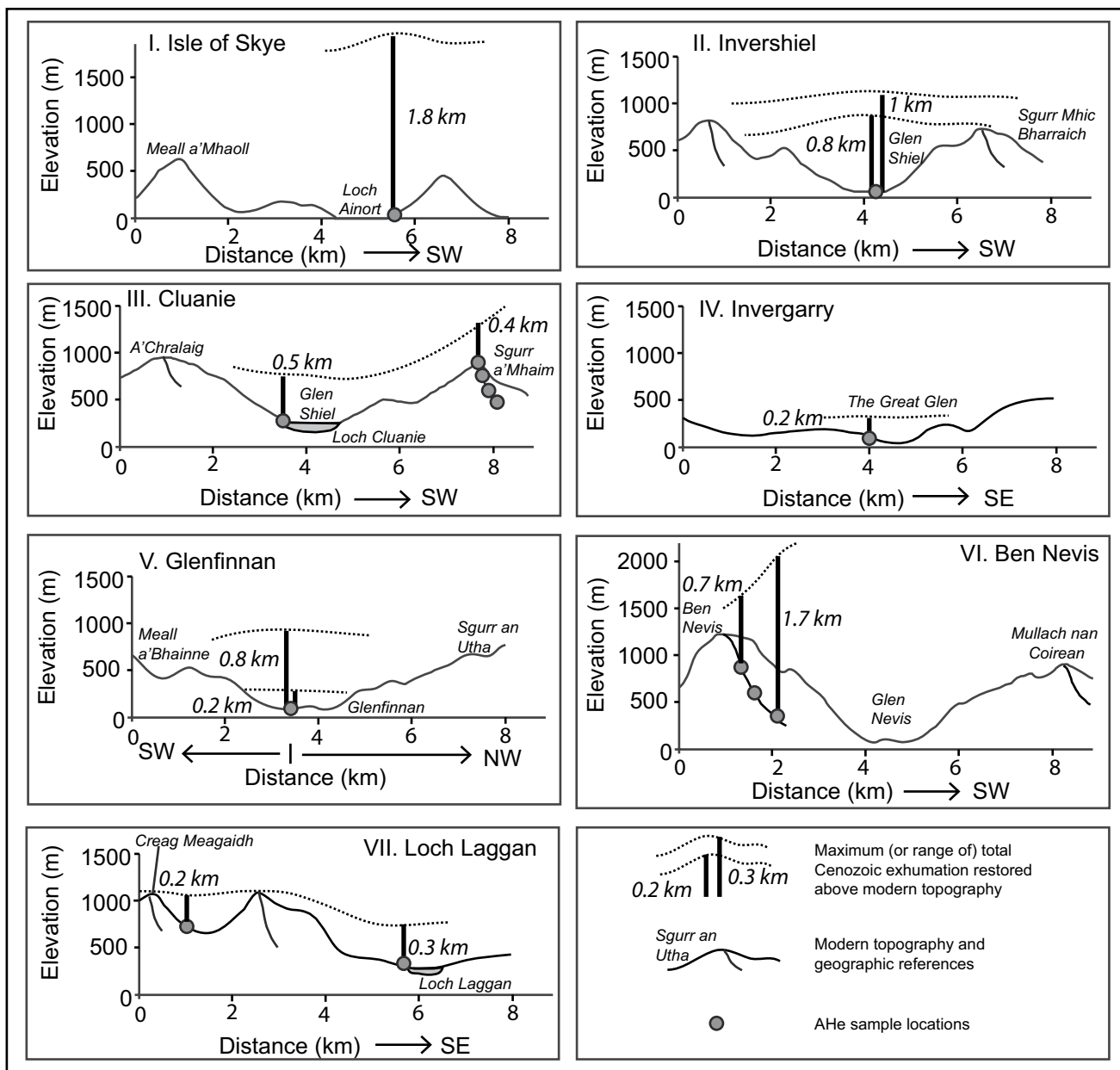


Figure 7. Maximum total Cenozoic exhumation depths across the study area (thick black vertical lines) were calculated based on the maximum Cenozoic temperature in the best-fit models for each sample site (with the exception of magmatic heating in the early Paleogene on the Isle of Skye and at Invershiel), a surface temperature of 10 °C, and a geothermal gradient of 30 °C km⁻¹. Cenozoic relief reconstructions (dotted line) restored above modern topography are based upon maximum exhumation depths and are not corrected for erosional isostasy, so they should be viewed as relative paleorelief rather than absolute elevations. AHe—apatite (U-Th)/He.

and a geothermal gradient of $30\text{ }^{\circ}\text{C km}^{-1}$. These estimates are inherently nonunique and should be considered maximum estimates, because the geothermal gradient in the early Cenozoic may have been higher (e.g., Thomson et al., 1999; Persano et al., 2007; Holford et al., 2010).

Restoration of these estimates of Cenozoic exhumation to the present-day topography illustrates potential Cenozoic relief development (Fig. 7). At Cluanie, Invergarry, Loch Laggan, Glenfinnan, and Invershiel, the restored exhumation is comparable or less than modern relief and results in smooth topography without deep U-shaped valleys. If a significant fraction of the Cenozoic exhumation occurred in the late Cenozoic, it is thus possible that onset of glacial erosion in the Pliocene–Pleistocene was responsible for significant relief production and generation of the modern landscape, as previously interpreted as the result of polythermal (selective linear) glacial erosion (Shackleton and Hall, 1984; Ballantyne, 2010; Fabel et al., 2012; Herman et al., 2013; Lowe and Walker, 2015; Fame et al., 2018); however, our data do not necessarily support this hypothesis. The higher estimates of exhumation from the Isle of Skye, Ben Nevis, and some estimates at Glenfinnan and Invershiel instead suggest greater Cenozoic exhumation than was required to produce modern-day relief, implying additional previous Cenozoic rock uplift and exhumation in addition to whatever glacial erosion produced (Fig. 7). Exhumation at the Isle of Skye may be overestimated as a result of elevated geothermal gradients during the Paleogene igneous event. However, in all cases, the magnitude of allowable Cenozoic exhumation does not permit excessive, i.e., $>1\text{ km}$, exhumation above the incision necessary to carve out the modern landscape, indicating that late Cenozoic glaciation in this setting did not result in the drastic acceleration of exhumation that has been observed in other tectonic settings (e.g., Herman et al., 2013).

Restoration of exhumation at Ben Nevis may also imply topographic inversion, in that more exhumation has occurred from lower-elevation samples than needed to incise valleys relative to neighboring peaks (Fig. 7). This may help explain why no forward models, which did not allow for such magnitudes of changing temperature offset and relief development, could recreate the observed age-elevation relationship there (Fig. 4). The need for this topographic inversion goes away if the Cenozoic geothermal gradient was as high as $60\text{ }^{\circ}\text{C km}^{-1}$ or if the highest-elevation samples were not completely reset during late Paleozoic to early Mesozoic reheating, however. More data and analysis of these results in three-dimensional thermo-kinematic models are ultimately required to refine these estimates.

Scotland's Heterogeneous Passive-Margin Evolution

New and existing thermochronometry from northwest Scotland is similar in a rough sense to the pattern of low-temperature ages observed along many other passive margins, in that apparent ages increase with distance from the coast or former rifted margin (Fig. 3). This pattern has been observed in numerous other passive margins and is typically explained in a context of erosional retreat of rift-flank escarpments, e.g., Eastern Brazilian Escarpment (Gallagher et al., 1994, 1995), Southeast Australian Escarpment (Moore et al., 1986; Persano et al., 2002, 2005), Western Ghats of India (Gunnell et al., 2003), and Blue Ridge Escarpment of the Appalachians (Spotila et al., 2004). In detail, however, it is clear that significant heterogeneity in cooling, burial, and exhumation is required to explain the data in Scotland. Similar heterogeneity has been observed in other passive margins as well, and it has been variously explained by erosional disequilibrium (Prince et al., 2010) or local tectonic reactivation associated with intraplate compression (e.g., Braun and Van Der Beek, 2004; Pe-Piper and Piper, 2004; West et al., 2008; Cogné et al., 2011; Amidon et al., 2016). Yet, the complexity of the thermal evolution of northwest Scotland, as now defined by extensive data of various kinds,

permits a more comprehensive accounting of the potential sources of heterogeneity in passive-margin evolution.

One insight from Scotland is the important role of nondenudational thermal events in local resetting or alteration of cooling histories. The importance of burial as a source of localized heating is illustrated by the late Paleozoic and early Mesozoic cooling history, during which post-Caledonian intracontinental basins were formed via extension and erosion and subsequently filled by sediment from neighboring highlands (Hall, 1991; Doré et al., 2002; Nielsen et al., 2009; Holford et al., 2010). While basin formation caused burial and heating at many locations across the Highlands, some areas, such as the Loch Laggan study site, remained elevated, escaping postorogenic burial and heating. Another source of localized heating in northwest Scotland was magmatism and underplating. Paleogene heating was confined to regions surrounding the Paleogene igneous complex (e.g., Anell et al., 2009), where it clearly impacted the thermal history.

The Northwest Scotland exhumation history also presents a case for intraplate fault reactivation due to far-field tectonic stresses. The short distances over which cooling histories vary may indicate the need for vertical separation along faults. The two major faults in the study area are the Great Glen fault and the Moine thrust (Fig. 3). Heating associated with Moine thrusting reached maximum temperatures in the Early Devonian (Johnson et al., 1985), and to our knowledge there has been no evidence found suggesting postorogenic reactivation of the Moine thrust. Alternatively, there is evidence that the Great Glen fault experienced Carboniferous to Permian and Cenozoic reactivation (Jolivet, 2007; Le Breton et al., 2013). AHe ages from near (i.e., $<7\text{ km}$) the Great Glen fault, both on the east side at Ben Nevis and the west side at Invergarry, as well as farther to the west of the fault at Invershiel, Glenfinnan, and Cluanie, all record a period of Carboniferous to Permian reheating, while the Loch Laggan site ($\sim 23\text{ km}$ southeast of the Great Glen fault) did not. If the Carboniferous to Permian sedimentary basins only formed near the reactivated Great Glen fault and to the northwest of it, this could have allowed for heating of some study sites while leaving the Loch Laggan site unburied. This could result from relative downward motion on the northwestern side of the fault and relative upward motion on the southeastern side. Such late Paleozoic independent motions of crustal blocks, possibly partitioned along secondary faults near the Great Glen corridor, have been previously suggested by Jolivet (2007).

Cenozoic exhumation on the Isle of Skye and Invershiel, expressed in features such as the Paleogene–Neogene scarp that exists along the Atlantic coast from the Cuillins to Cape Wrath as a result of warping of Scotland's Atlantic margin (Fig. 2; Hall and Bishop, 2002), may have been driven by Cenozoic intraplate compression inboard of the Mid-Atlantic Ridge and Alpine orogen (Hall and Bishop, 2002; Jolivet, 2007; Holford et al., 2010). Such intraplate compression has also been attributed to Cenozoic reactivation of the Great Glen fault (Le Breton et al., 2013).

Climate-driven spatial variation in denudation may represent an additional source of heterogeneity in the cooling history of northwest Scotland, although this does not appear to have influenced the differential cooling histories we observed in our study areas. The topographic history of the region is not known, but the topography is consistent with spatially variable glacial erosion, as some regions exhibit rounded, low-relief forms, and others exhibit deep glacial valleys and sharp intervening ridges (e.g., Sugden, 1968; Hall and Sugden, 1987; Jansen et al., 2011; Fabel et al., 2012; Whitbread et al., 2015; Fame et al., 2018). The degree to which glaciers modified the landscape likely depended on local preglacial topography (mean elevation and relief), lithology, and ice dynamics (e.g., Hall and Sugden, 1987; Kirkbride and Matthews, 1997; Hall et al., 2013). Given that these factors differ across the study area, it is likely that the

magnitude of late Cenozoic glacially driven denudation was spatially variable, thus representing another potential cause of heterogeneity in the evolution of this passive margin. Although our data do not capture such a signal, they are still valuable in showing that the total magnitude of late Cenozoic glacial denudation was limited to much less than 1 km. This indicates that onset of glacial climate was much less of a factor in altering evolution of this passive margin than tectonics.

CONCLUSIONS

The history of Scotland's passive margin can be interpreted as resulting from multiple stages of postorogenic burial and exhumation that were spatially heterogeneous over short distances (~20–100 km). Apparent AHe ages taken from seven field sites range from 31.2 ± 5.2 Ma to 363.4 ± 31.4 Ma (Table 1; Fig. 3) within ~100 km across the western Scottish Highlands (Figs. 2 and 3). Thermal modeling indicates that these data require different combinations of post-Caledonian heating and cooling events occurring in the (1) late Paleozoic to early Mesozoic, (2) Late Jurassic to Early Cretaceous, (3) Late Cretaceous, (4) Paleogene, and (5) Neogene (Fig. 6; Table 2). The short distances over which other periods of heterogeneous burial and exhumation vary indicate the influence of vertical separation along the Great Glen fault, margin tilting during rifting, and far-field effects of Alpine compression. Emplacement of the Paleogene igneous complex can locally explain Paleogene heating and cooling events. Varying magnitudes of low to moderate (i.e., <1 km) total Cenozoic exhumation across the study area suggest that the onset of glacial climate in the late Cenozoic and preexisting paleotopography may also have been factors in controlling exhumation of Scotland's passive margin. Our results, which build on the already extensive constraints for the thermal evolution of this region, provide new insights into the importance of spatially heterogeneous intracontinental basin formation and exhumation across reactivated faults in the postorogenic thermal evolution of passive margins.

ACKNOWLEDGMENTS

We are grateful for helpful discussions of ideas with Josh Valentino, Cody Mason, Joe Cochran, and Jenny Arkle. We would like to thank Kurt Stüwe, Paul Green, Adrian Hall, and an unnamed reviewer for their input on earlier versions of the manuscript. Thanks go to Nick Fylstra and Marissa Tremblay for help with $^4\text{He}/^3\text{He}$ analysis at the Berkeley Geochronology Center and Marc Caffee for his help in the field. This study was funded by National Science Foundation Geomorphology grants EAR-003137015 and EAR-1123643.

REFERENCES CITED

Amidon, W., Roden-Tice, M., Anderson, A., McKeon, R., and Shuster, D., 2016, Late Cretaceous unroofing of the White Mountains, New Hampshire, USA: An episode of passive margin rejuvenation? *Geology*, v. 44, p. 415–418, <https://doi.org/10.1130/G37429.1>.

Anell, I., Thybo, H., and Artemieva, I., 2009, Cenozoic uplift and subsidence in the North Atlantic region: Geological evidence revisited: *Tectonophysics*, v. 474, no. 1, p. 78–105, <https://doi.org/10.1016/j.tecto.2009.04.006>.

Ballantyne, C.K., 2010, Extent and deglacial chronology of the last British–Irish ice sheet: Implications of exposure dating using cosmogenic isotopes: *Journal of Quaternary Science*, v. 25, no. 4, p. 515–534, <https://doi.org/10.1002/jqs.1310>.

Ballantyne, C.K., and Stone, J.O., 2012, Did large ice caps persist on low ground in north-west Scotland during the Lateglacial interstade? *Journal of Quaternary Science*, v. 27, no. 3, p. 297–306, <https://doi.org/10.1002/jqs.1544>.

Braun, J., and Van Der Beek, P., 2004, Evolution of passive margin escarpments: What can we learn from low-temperature thermochronology? *Journal of Geophysical Research—Earth Surface*, v. 109, F4009, <https://doi.org/10.1029/2004JF000147>.

British Geological Survey, 2012, *The British Geological Survey Lexicon of Named Rock Units: UK*, British Geological Survey, <http://www.bgs.ac.uk/Lexicon>.

Clift, P., Carter, A., and Hurford, A., 1998, The erosional and uplift history of NE Atlantic passive margins: Constraints on a passing plume: *Journal of the Geological Society [London]*, v. 155, no. 5, p. 787–800, <https://doi.org/10.1144/gsjgs.155.5.0787>.

Cogné, N., Gallagher, K., and Cobbold, P.R., 2011, Post-rift reactivation of the onshore margin of southeast Brazil: Evidence from apatite (U-Th)/He and fission-track data: *Earth and Planetary Science Letters*, v. 309, no. 1, p. 118–130, <https://doi.org/10.1016/j.epsl.2011.06.025>.

Cogné, N., Doepke, D., Chew, D., Stuart, F.M., and Mark, C., 2016, Measuring plume-related exhumation of the British Isles in early Cenozoic times: *Earth and Planetary Science Letters*, v. 456, p. 1–15, <https://doi.org/10.1016/j.epsl.2016.09.053>.

Dodson, M.H., 1973, Closure temperature in cooling geochronological and petrological systems: *Contributions to Mineralogy and Petrology*, v. 40, no. 3, p. 259–274, <https://doi.org/10.1007/BF00373790>.

Doré, A., Lundin, E., Jensen, L., Birkeland, Ø., Eliassen, P., and Fichler, C., 1999, Principal tectonic events in the evolution of the northwest European Atlantic margin, in Fleet, A.J., and Boldy, S.A.R., eds., *Proceedings of the Petroleum Geology Conference 1999*, Volume 5: Geological Society, London, p. 41–61.

Doré, A., Cartwright, J., Stoker, M., Turner, J., and White, N., 2002, Exhumation of the North Atlantic margin: Introduction and background, in Doré, A., Cartwright, J., Stoker, M., Turner, J., and White, N., *Exhumation of the North Atlantic Margin: Timing, Mechanisms, and Implications for Petroleum Exploration: Geological Society, London, Special Publication 196*, p. 1–12, <https://doi.org/10.1144/GSL.SP2002.196.01.01>.

Ehlers, T.A., and Farley, K.A., 2003, Apatite (U-Th)/He thermochronometry: Methods and applications to problems in tectonic and surface processes: *Earth and Planetary Science Letters*, v. 206, no. 1, p. 1–14, [https://doi.org/10.1016/S0012-821X\(02\)01069-5](https://doi.org/10.1016/S0012-821X(02)01069-5).

Evans, D., Stoker, M., and Shannon, P., 2005, The STRATAGEM project: Stratigraphic development of the glaciated European margin: *Marine and Petroleum Geology*, v. 22, no. 9, p. 969–976, <https://doi.org/10.1016/j.marpetgeo.2005.02.002>.

Fabel, D., Ballantyne, C.K., and Xu, S., 2012, Trilines, blockfields, mountain-top erratics and the vertical dimensions of the last British–Irish ice sheet in NW Scotland: *Quaternary Science Reviews*, v. 55, p. 91–102, <https://doi.org/10.1016/j.quascirev.2012.09.002>.

Fame, M.L., Owen, L.A., Spotila, J.A., Dortch, J.M., and Caffee, M.W., 2018, Tracking paraglacial sediment with cosmogenic ^{10}Be using an example from the northwest Scottish Highlands: *Quaternary Science Reviews*, v. 182, p. 20–36, <https://doi.org/10.1016/j.quascirev.2017.12.017>.

Farley, K., 2000, Helium diffusion from apatite: General behavior as illustrated by Durango fluorapatite: *Journal of Geophysical Research—Solid Earth (1978–2012)*, v. 105, no. B2, p. 2903–2914.

Farley, K., and Stockli, D.F., 2002, (U-Th)/He dating of phosphates: Apatite, monazite, and xenotime: *Reviews in Mineralogy and Geochemistry*, v. 48, no. 1, p. 559–577, <https://doi.org/10.2138/rmg.2002.48.15>.

Farley, K., Wolf, R., and Silver, L., 1996, The effects of long alpha-stopping distances on (U-Th)/He ages: *Geochimica et Cosmochimica Acta*, v. 60, no. 21, p. 4223–4229, [https://doi.org/10.1016/S0016-7037\(96\)00193-7](https://doi.org/10.1016/S0016-7037(96)00193-7).

Farley, K., Shuster, D., Watson, E., Wanser, K., and Balco, G., 2010, Numerical investigations of apatite $^4\text{He}/^3\text{He}$ thermochronometry: *Geochemistry Geophysics Geosystems*, v. 11, Q10001, <https://doi.org/10.1029/2010GC003243>.

Flowers, R.M., and Kelley, S.A., 2011, Interpreting data dispersion and “inverted” dates in apatite (U-Th)/He and fission-track datasets: An example from the US midcontinent: *Geochimica et Cosmochimica Acta*, v. 75, no. 18, p. 5169–5186, <https://doi.org/10.1016/j.gca.2011.06.016>.

Flowers, R.M., Shuster, D., Wernicke, B., and Farley, K., 2007, Radiation damage control on apatite (U-Th)/He dates from the Grand Canyon region, Colorado Plateau: *Geology*, v. 35, no. 5, p. 447–450, <https://doi.org/10.1130/G23471A.1>.

Flowers, R.M., Ketcham, R.A., Shuster, D.L., and Farley, K.A., 2009, Apatite (U-Th)/He thermochronometry using a radiation damage accumulation and annealing model: *Geochimica et Cosmochimica Acta*, v. 73, no. 8, p. 2347–2365, <https://doi.org/10.1016/j.gca.2009.01.015>.

Gallagher, K., 2012, Transdimensional inverse thermal history modeling for quantitative thermochronology: *Journal of Geophysical Research—Solid Earth (1978–2012)*, v. 117, no. B2, B02408, <https://doi.org/10.1029/2011JB008825>.

Gallagher, K., and Brown, R., 1999, The Mesozoic denudation history of the Atlantic margins of southern Africa and southeast Brazil and the relationship to offshore sedimentation: *Geological Society, London, Special Publications*, v. 153, no. 1, p. 41–53.

Gallagher, K., Hawkesworth, C., and Mantovani, M., 1994, The denudation history of the onshore continental margin of SE Brazil inferred from apatite fission track data: *Journal of Geophysical Research—Solid Earth*, v. 99, no. B9, p. 18,117–18,145, <https://doi.org/10.1029/94JB00661>.

Gallagher, K., Hawkesworth, C., and Mantovani, M., 1995, Denudation, fission track analysis and the long-term evolution of passive margin topography: Application to the southeast Brazilian margin: *Journal of South American Earth Sciences*, v. 8, no. 1, p. 65–77, [https://doi.org/10.1016/0895-9811\(94\)00042-Z](https://doi.org/10.1016/0895-9811(94)00042-Z).

Gallagher, K., Stephenson, J., Brown, R., Holmes, C., and Fitzgerald, P., 2005, Low temperature thermochronology and modeling strategies for multiple samples 1: Vertical profiles: *Earth and Planetary Science Letters*, v. 237, no. 1, p. 193–208, <https://doi.org/10.1016/j.epsl.2005.06.025>.

George, T.N., 1966, Geomorphic evolution in Hebridean Scotland: *Scottish Journal of Geology*, v. 2, no. 1, p. 1–34.

Golledge, N.R., 2010, Glaciation of Scotland during the Younger Dryas stadial: A review: *Journal of Quaternary Science*, v. 25, no. 4, p. 550–566, <https://doi.org/10.1002/jqs.1319>.

Green, P., and Duddy, I., 2006, Interpretation of apatite (U-Th)/He ages and fission track ages from cratons: *Earth and Planetary Science Letters*, v. 244, no. 3, p. 541–547, <https://doi.org/10.1016/j.epsl.2006.02.024>.

Green, P., and Duddy, I., 2010, Synchronous exhumation events around the Arctic including examples from Barents Sea and Alaska North Slope, in Vining, B.A., and Pickering, S.C., eds., *Proceedings of the Petroleum Geology Conference 2010*, Volume 7: Geological Society, London, p. 633–644.

Green, P.F., Crowhurst, P.V., Duddy, I.R., Japsen, P., and Holford, S.P., 2006, Conflicting (U-Th)/He and fission track ages in apatite: Enhanced He retention, not anomalous annealing behaviour: *Earth and Planetary Science Letters*, v. 250, no. 3, p. 407–427, <https://doi.org/10.1016/j.epsl.2006.08.022>.

Gunnell, Y., Gallagher, K., Carter, A., Widdowson, M., and Hurford, A., 2003, Denudation history of the continental margin of western peninsular India since the early Mesozoic—Reconciling apatite fission-track data with geomorphology: *Earth and Planetary Science Letters*, v. 215, no. 1, p. 187–201, [https://doi.org/10.1016/S0012-821X\(03\)00380-7](https://doi.org/10.1016/S0012-821X(03)00380-7).

- Hall, A., 1991, Pre-Quaternary landscape evolution in the Scottish Highlands: *Transactions of the Royal Society of Edinburgh—Earth Sciences*, v. 82, no. 1, p. 1–26, <https://doi.org/10.1017/S0263593300007495>.
- Hall, A., and Bishop, P., 2002, Scotland's denudational history: An integrated view of erosion and sedimentation at an uplifted passive margin, in Doré, A., Cartwright, J., Stoker, M., Turner, J., and White, N., *Exhumation of the North Atlantic Margin: Timing, Mechanisms, and Implications for Petroleum Exploration*: Geological Society, London, Special Publication 196, p. 271–290, <https://doi.org/10.1144/GSL.SP.2002.196.01.15>.
- Hall, A., and Sugden, D.E., 1987, Limited modification of mid-latitude landscapes by ice sheets: The case of northeast Scotland: *Earth Surface Processes and Landforms*, v. 12, no. 5, p. 531–542, <https://doi.org/10.1002/esp.3290120510>.
- Hall, A.M., Ebert, K., and Hättestrand, C., 2013, Pre-glacial landform inheritance in a glaciated shield landscape: *Geografiska Annaler, ser. A, Physical Geography*, v. 95, no. 1, p. 33–49, <https://doi.org/10.1111/j.1468-0459.2012.00477.x>.
- Herman, F., Seward, D., Valla, P.G., Carter, A., Kohn, B., Willett, S.D., and Ehlers, T.A., 2013, Worldwide acceleration of mountain erosion under a cooling climate: *Nature*, v. 504, no. 7480, p. 423–426, <https://doi.org/10.1038/nature12877>.
- Holford, S.P., Green, P.F., Duddy, I.R., Turner, J.P., Hillis, R.R., and Stoker, M.S., 2009, Regional intraplate exhumation episodes related to plate-boundary deformation: *Geological Society of America Bulletin*, v. 121, no. 11–12, p. 1611–1628, <https://doi.org/10.1130/B26481.1>.
- Holford, S.P., Green, P.F., Hillis, R.R., Underhill, J.R., Stoker, M.S., and Duddy, I.R., 2010, Multiple post-Caledonian exhumation episodes across NW Scotland revealed by apatite fission-track analysis: *Journal of the Geological Society [London]*, v. 167, no. 4, p. 675–694, <https://doi.org/10.1144/0016-76492009-167>.
- Huntington, K.W., Ehlers, T.A., Hodges, K.V., and Whipp, D.M., 2007, Topography, exhumation pathway, age uncertainties, and the interpretation of thermochronometer data: *Tectonics*, v. 26, <https://doi.org/10.1029/2007TC002108>.
- Jansen, J.D., Fabel, D., Bishop, P., Xu, S., Schnabel, C., and Codilean, A.T., 2011, Does decreasing paraclastic sediment supply slow knickpoint retreat?: *Geology*, v. 39, no. 6, p. 543–546, <https://doi.org/10.1130/G32018.1>.
- Japsen, P., Bonow, J.M., Green, P.F., Chalmers, J.A., and Lidmar-Bergström, K., 2006, Elevated, passive continental margins: Long-term highs or Neogene uplifts? New evidence from West Greenland: *Earth and Planetary Science Letters*, v. 248, no. 1, p. 330–339, <https://doi.org/10.1016/j.epsl.2006.05.036>.
- Japsen, P., Bonow, J.M., Green, P.F., Chalmers, J.A., and Lidmar-Bergström, K., 2009, Formation, uplift and dissection of planation surfaces at passive continental margins—A new approach: *Earth Surface Processes and Landforms*, v. 34, no. 5, p. 683–699, <https://doi.org/10.1002/esp.1766>.
- Johnson, M., Kelley, S., Oliver, G., and Winter, D., 1985, Thermal effects and timing of thrusting in the Moine thrust zone: *Journal of the Geological Society [London]*, v. 142, no. 5, p. 863–873, <https://doi.org/10.1144/gsjgs.142.5.0863>.
- Jolivet, M., 2007, Histoire de la dénudation dans le corridor du loch Ness (Écosse): *Mouvements verticaux différentiels le long de la Great Glen fault*: *Comptes Rendus Geoscience*, v. 339, no. 2, p. 121–131, <https://doi.org/10.1016/j.crte.2006.12.005>.
- Kirkbride, M., and Matthews, D., 1997, The role of fluvial and glacial erosion in landscape evolution: The Ben Ohau Range, New Zealand: *Earth Surface Processes and Landforms*, v. 22, no. 3, p. 317–327, [https://doi.org/10.1002/\(SICI\)1096-9837\(199703\)22:3<317::AID-ESP760>3.0.CO;2-I](https://doi.org/10.1002/(SICI)1096-9837(199703)22:3<317::AID-ESP760>3.0.CO;2-I).
- Knott, S., Burchell, M., Jolley, E., and Fraser, A., 1993, Mesozoic to Cenozoic plate reconstructions of the North Atlantic and hydrocarbon plays of the Atlantic margins, in Parker, J.R., ed., *Proceedings of the Petroleum Geology Conference 1993, Volume 4*: Geological Society, London, p. 953–974.
- Le Breton, E., Cobbold, P., Dauteuil, O., and Lewis, G., 2012, Variations in amount and direction of seafloor spreading along the northeast Atlantic Ocean and resulting deformation of the continental margin of northwest Europe: *Tectonics*, v. 31, TC5006, <https://doi.org/10.1029/2011TC003087>.
- Le Breton, E., Cobbold, P.R., and Zanella, A., 2013, Cenozoic reactivation of the Great Glen fault, Scotland: Additional evidence and possible causes: *Journal of the Geological Society [London]*, v. 170, no. 3, p. 403–415, <https://doi.org/10.1144/jgs2012-067>.
- Lowe, J.J., and Walker, M.J., 2015, *Reconstructing Quaternary Environments*: Routledge, 568 p.
- McDowell, F.W., McIntosh, W.C., and Farley, K.A., 2005, A precise ^{40}Ar – ^{39}Ar reference age for the Durango apatite (U–Th)/He and fission-track dating standard: *Chemical Geology*, v. 214, no. 3, p. 249–263.
- McKeon, R.E., Zeitler, P.K., Pazzaglia, F.J., Idleman, B.D., and Enkelmann, E., 2014, Decay of an old orogen: Inferences about Appalachian landscape evolution from low-temperature thermochronology: *Geological Society of America Bulletin*, v. 126, no. 1–2, p. 31–46, <https://doi.org/10.1130/B30808.1>.
- McKerrow, W., Mac Niocaill, C., and Dewey, J., 2000, The Caledonian orogeny redefined: *Journal of the Geological Society [London]*, v. 157, no. 6, p. 1149–1154, <https://doi.org/10.1144/jgs.157.6.1149>.
- Met-Office, U.K., 2013, Scotland Mean Temperature (Degrees C), Areal series, starting from 1910: UK, Met-Office, <http://www.metoffice.gov.uk/climate/uk/datasets/Tmean/ranked/Scotland.txt> (accessed July 2013).
- Montgomery, D.R., 1994, Valley incision and the uplift of mountain peaks: *Journal of Geophysical Research*, v. 99, no. B7, p. 13,913–13,921, <https://doi.org/10.1029/94JB00122>.
- Moore, M.E., Gleadow, A.J., and Lovering, J.F., 1986, Thermal evolution of rifted continental margins: New evidence from fission tracks in basement apatites from southeastern Australia: *Earth and Planetary Science Letters*, v. 78, no. 2, p. 255–270, [https://doi.org/10.1016/0012-821X\(86\)90066-X](https://doi.org/10.1016/0012-821X(86)90066-X).
- Nielsen, S.B., Gallagher, K., Leighton, C., Balling, N., Svenningsen, L., Jacobsen, B.H., Thomsen, E., Nielsen, O.B., Heilmann-Clausen, C., and Egholm, D.L., 2009, The evolution of western Scandinavian topography: A review of Neogene uplift versus the ICE (isostasy–climate–erosion) hypothesis: *Journal of Geodynamics*, v. 47, no. 2, p. 72–95, <https://doi.org/10.1016/j.jog.2008.09.001>.
- Pe-Piper, G., and Piper, D.J., 2004, The effects of strike-slip motion along the Cobequid–Chedabucto–southwest Grand Banks fault system on the Cretaceous–Tertiary evolution of Atlantic Canada: *Canadian Journal of Earth Sciences*, v. 41, no. 7, p. 799–808, <https://doi.org/10.1139/e04-022>.
- Persano, C., Stuart, F.M., Bishop, P., and Barfod, D.N., 2002, Apatite (U–Th)/He age constraints on the development of the Great Escarpment on the southeastern Australian passive margin: *Earth and Planetary Science Letters*, v. 200, no. 1, p. 79–90, [https://doi.org/10.1016/S0012-821X\(02\)00614-3](https://doi.org/10.1016/S0012-821X(02)00614-3).
- Persano, C., Stuart, F.M., Bishop, P., and Dempster, T.J., 2005, Deciphering continental breakup in eastern Australia using low-temperature thermochronometers: *Journal of Geophysical Research—Solid Earth*, v. 110, B12405, <https://doi.org/10.1029/2004JB003325>.
- Persano, C., Barfod, D.N., Stuart, F.M., and Bishop, P., 2007, Constraints on early Cenozoic underplating-driven uplift and denudation of western Scotland from low temperature thermochronometry: *Earth and Planetary Science Letters*, v. 263, no. 3, p. 404–419, <https://doi.org/10.1016/j.epsl.2007.09.016>.
- Praeg, D., Stoker, M., Shannon, P., Ceramicola, S., Hjelstuen, B., Laberg, J., and Mathiesen, A., 2005, Episodic Cenozoic tectonism and the development of the NW European 'passive' continental margin: *Marine and Petroleum Geology*, v. 22, no. 9, p. 1007–1030, <https://doi.org/10.1016/j.marpetgeo.2005.03.014>.
- Prince, P.S., Spotila, J.A., and Henika, W.S., 2010, New physical evidence of the role of stream capture in active retreat of the Blue Ridge Escarpment, Southern Appalachians: *Geomorphology*, v. 123, no. 3, p. 305–319, <https://doi.org/10.1016/j.geomorph.2010.07.023>.
- Reiners, P.W., and Brandon, M.T., 2006, Using thermochronology to understand orogenic erosion: *Annual Review of Earth and Planetary Sciences*, v. 34, p. 419–466, <https://doi.org/10.1146/annurev.earth.34.031405.125202>.
- Reiners, P.W., and Nicolescu, S., 2006, Measurement of Parent Nuclides for (U–Th)/He Chronometry by Solution Sector ICP-MS: Arizona Radiogenic Helium Dating Laboratory (ARHDL) Report 1, 33 p.
- Roden-Tice, M.K., and Tice, S.J., 2005, Regional-scale mid-Jurassic to Late Cretaceous unroofing from the Adirondack Mountains through central New England based on apatite fission-track and (U–Th)/He thermochronology: *The Journal of Geology*, v. 113, no. 5, p. 535–552, <https://doi.org/10.1086/431908>.
- Rowley, D.B., Forte, A.M., Moucha, R., Mitrovica, J.X., Simmons, N.A., and Grand, S.P., 2013, Dynamic topography change of the eastern United States since 3 million years ago: *Science*, v. 340, no. 6140, p. 1560–1563.
- Schildgen, T.F., Balco, G., and Shuster, D.L., 2010, Canyon incision and knickpoint propagation recorded by apatite $^{4}\text{He}/^{3}\text{He}$ thermochronometry: *Earth and Planetary Science Letters*, v. 293, no. 3, p. 377–387, <https://doi.org/10.1016/j.epsl.2010.03.009>.
- Shackleton, N., and Hall, M., 1984, Oxygen and carbon isotope stratigraphy of Deep Sea Drilling Project Hole 552A: Plio-Pleistocene glacial history, in Roberts, D.G., and Schnittker, D., eds., *Initial Reports of the Deep Sea Drilling Project, Volume 81*: Washington, D.C., U.S. Government Printing Office, p. 599–609.
- Shuster, D.L., and Farley, K.A., 2004, $^{4}\text{He}/^{3}\text{He}$ thermochronometry: *Earth and Planetary Science Letters*, v. 217, no. 1, p. 1–17, [https://doi.org/10.1016/S0012-821X\(03\)00595-8](https://doi.org/10.1016/S0012-821X(03)00595-8).
- Shuster, D.L., and Farley, K.A., 2005, $^{4}\text{He}/^{3}\text{He}$ thermochronometry: Theory, practice, and potential complications: *Reviews in Mineralogy and Geochemistry*, v. 58, no. 1, p. 181–203, <https://doi.org/10.2138/rmg.2005.58.7>.
- Shuster, D., Farley, K., Sisterson, J., and Burnett, D., 2003, $^{4}\text{He}/^{3}\text{He}$ thermochronometry: *Geochimica et Cosmochimica Acta*, v. 67, supplement, p. 436.
- Shuster, D.L., Flowers, R.M., and Farley, K.A., 2006, The influence of natural radiation damage on helium diffusion kinetics in apatite: *Earth and Planetary Science Letters*, v. 249, no. 3, p. 148–161, <https://doi.org/10.1016/j.epsl.2006.07.028>.
- Spotila, J.A., 2005, Applications of low-temperature thermochronometry to quantification of recent exhumation in mountain belts: *Reviews in Mineralogy and Geochemistry*, v. 58, no. 1, p. 449–466, <https://doi.org/10.2138/rmg.2005.58.17>.
- Spotila, J.A., and Berger, A.L., 2010, Exhumation at orogenic indenter corners under long-term glacial conditions: Example of the St. Elias orogen, Southern Alaska: *Tectonophysics*, v. 490, no. 3, p. 241–256.
- Spotila, J.A., Bank, G.C., Reiners, P.W., Naeser, C.W., Naeser, N.D., and Henika, B.S., 2004, Origin of the Blue Ridge Escarpment along the passive margin of eastern North America: *Basin Research*, v. 16, no. 1, p. 41–63, <https://doi.org/10.1111/j.1365-2117.2003.00219.x>.
- Stoker, M., 2002, Late Neogene development of the UK Atlantic margin, in Doré, A., Cartwright, J., Stoker, M., Turner, J., and White, N., *Exhumation of the North Atlantic Margin: Timing, Mechanisms, and Implications for Petroleum Exploration*: Geological Society, London, Special Publication 196, p. 313–329, <https://doi.org/10.1144/GSL.SP.2002.196.01.17>.
- Stoker, M., Hoult, R., Nielsen, T., Hjelstuen, B., Laberg, J., Shannon, P., Praeg, D., Mathiesen, A., Van Weering, T., and McDonnell, A., 2005a, Sedimentary and oceanographic responses to early Neogene compression on the NW European margin: *Marine and Petroleum Geology*, v. 22, no. 9, p. 1031–1044, <https://doi.org/10.1016/j.marpetgeo.2005.01.009>.
- Stoker, M., Praeg, D., Shannon, P., Hjelstuen, B., Laberg, J., Nielsen, T., Van Weering, T., Sejrup, H., and Evans, D., 2005b, Neogene evolution of the Atlantic continental margin of NW Europe (Lofoten Islands to SW Ireland): Anything but passive, in Dore, A.G., and Vining, B.A., eds., *Proceedings of the 6th Petroleum Geology Conference: North West Europe and Global Perspectives*: Geological Society, London, p. 1057–1076.
- Stoker, M.S., Praeg, D., Hjelstuen, B.O., Laberg, J.S., Nielsen, T., and Shannon, P.M., 2005c, Neogene stratigraphy and the sedimentary and oceanographic development of the NW European Atlantic margin: *Marine and Petroleum Geology*, v. 22, no. 9, p. 977–1005, <https://doi.org/10.1016/j.marpetgeo.2004.11.007>.

- Stoker, M.S., Holford, S.P., Hillis, R.R., Green, P.F., and Duddy, I.R., 2010, Cenozoic post-rift sedimentation off northwest Britain: Recording the detritus of episodic uplift on a passive continental margin: *Geology*, v. 38, no. 7, p. 595–598, <https://doi.org/10.1130/G30881.1>.
- Sugden, D., 1968, The selectivity of glacial erosion in the Cairngorm Mountains, Scotland: *Transactions of the Institute of British Geographers*, no. 45, p. 79–92, <https://doi.org/10.2307/621394>.
- Taylor, J.P., and Fitzgerald, P.G., 2011, Low-temperature thermal history and landscape development of the eastern Adirondack Mountains, New York: Constraints from apatite fission-track thermochronology and apatite (U-Th)/He dating: *Geological Society of America Bulletin*, v. 123, no. 3–4, p. 412–426, <https://doi.org/10.1130/B30138.1>.
- Thomson, K., Underhill, J., Green, P., Bray, R., and Gibson, H., 1999, Evidence from apatite fission track analysis for the post-Devonian burial and exhumation history of the northern Highlands, Scotland: *Marine and Petroleum Geology*, v. 16, no. 1, p. 27–39, [https://doi.org/10.1016/S0264-8172\(98\)00064-6](https://doi.org/10.1016/S0264-8172(98)00064-6).
- Tranel, L.M., Spotila, J.A., Kowalewski, M.J., and Waller, C.M., 2011, Spatial variation of erosion in a small, glaciated basin in the Teton Range, Wyoming, based on detrital apatite (U-Th)/He thermochronology: *Basin Research*, v. 23, no. 5, p. 571–590.
- Tremblay, M.M., Fox, M., Schmidt, J.L., Tripathy-Lang, A., Wielicki, M.M., Harrison, T.M., Zeitler, P.K., and Shuster, D.L., 2015, Erosion in southern Tibet shut down at ~10 Ma due to enhanced rock uplift within the Himalaya: *Proceedings of the National Academy of Sciences of the United States of America*, v. 112, no. 39, p. 12,030–12,035, <https://doi.org/10.1073/pnas.1515652112>.
- Valentino, J.D., Spotila, J.A., Owen, L.A., and Buscher, J.T., 2016, Rock uplift at the transition from flat-slab to normal subduction: The Kenai Mountains, southeast Alaska: *Tectonophysics*, v. 671, p. 63–75, <https://doi.org/10.1016/j.tecto.2016.01.022>.
- Watson, J., 1985, Northern Scotland as an Atlantic–North Sea divide: *Journal of the Geological Society [London]*, v. 142, no. 2, p. 221–243, <https://doi.org/10.1144/gsjgs.142.2.0221>.
- West, D.P., Pinet, N., Roden-Tice, M.K., Potter, J.K., and Barnard, N.Q., 2008, Assessing the role of orogen-parallel faulting in post-orogenic exhumation: Low-temperature thermochronology across the Norumbega fault system, Maine: *Canadian Journal of Earth Sciences*, v. 45, no. 3, p. 287–301, <https://doi.org/10.1139/E07-073>.
- Whitbread, K., Jansen, J., Bishop, P., and Attal, M., 2015, Substrate, sediment, and slope controls on bedrock channel geometry in postglacial streams: *Journal of Geophysical Research–Earth Surface*, v. 120, no. 5, p. 779–798, <https://doi.org/10.1002/2014JF003295>.
- Wolf, R., Farley, K., and Kass, D., 1998, Modeling of the temperature sensitivity of the apatite (U-Th)/He thermochronometer: *Chemical Geology*, v. 148, no. 1, p. 105–114, [https://doi.org/10.1016/S0009-2541\(98\)00024-2](https://doi.org/10.1016/S0009-2541(98)00024-2).
- Ziegler, P., 1981, Evolution of sedimentary basins in North-West Europe, *in* Illing, L.V., and Hobson, G.D., eds., *The Petroleum geology of the continental shelf of north-west Europe*: London, Heyden, p. 3–39.

MANUSCRIPT RECEIVED 7 MAY 2017

REVISED MANUSCRIPT RECEIVED 10 JANUARY 2018

MANUSCRIPT ACCEPTED 27 FEBRUARY 2018